In situ MAS NMR spectroscopy: State of the art and applications

Michael Hunger
Institute of Chemical Technology
University of Stuttgart

KU Leuven, Belgium
March 19, 2014

Isotopes interesting for solid-state NMR in heterogeneous catalysis

(nuclear spin, relative sensitivity in comparison with ^{1}H)

^{1}H (1/2, 1.00), ^{2}H (1, 1.4×10^{-6})

^{13}C (1/2, 1.8×10^{-4}), ^{15}N (1/2, 3.8×10^{-6})

^{31}P (1/2, 6.6×10^{-2})

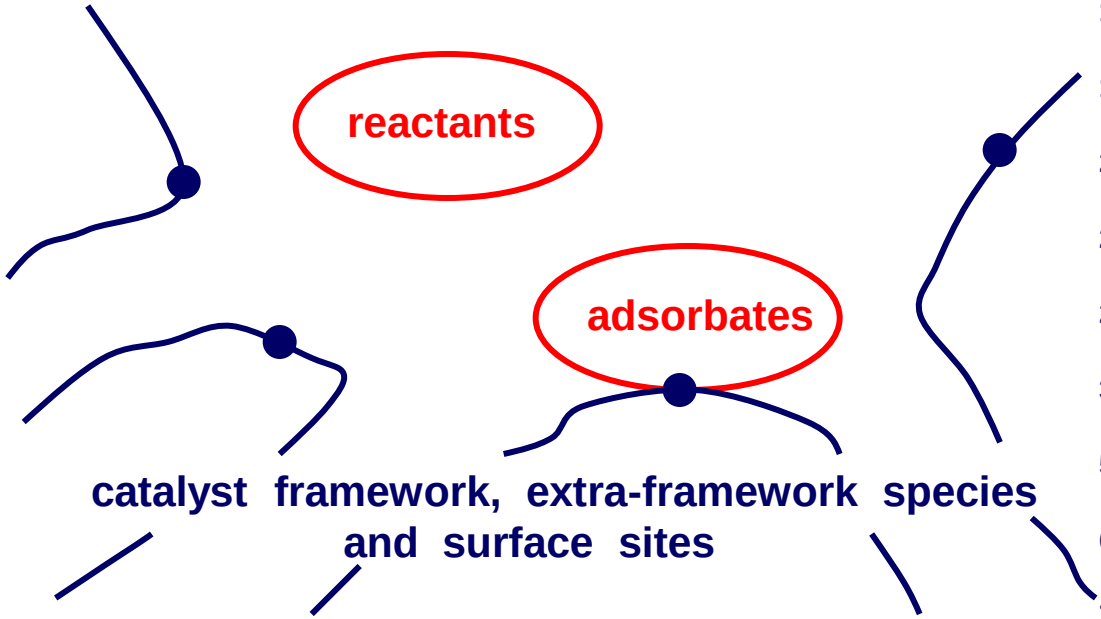

^{7}Li (3/2, 0.27)

^{11}B (3/2, 0.13)

^{17}O (5/2, 1.1×10^{-5})

^{23}Na (3/2, 9.2×10^{-2})

^{27}Al (5/2, 0.21)

^{29}Si (1/2, 3.7×10^{-4})

^{31}P (1/2, 6.6×10^{-2})

^{51}V (7/2, 0.38)

^{67}Zn (5/2, 1.2×10^{-2})

^{71}Ga (3/2, 5.6×10^{-2})

^{133}Cs (7/2, 4.7×10^{-2})

Specific problems of solid-state NMR spectroscopy

Magnetization M_0, Curie's law:

$$M_0 = \frac{N\,\gamma^2\,h^2\,I\,(I+1)\,B_0}{(2\pi)^2\,3\,k_B\,T}$$

detection limit of solid-state NMR is ca. N = 10 µmol spins per gram for ^{1}H nuclei at room temperature

magnetization M_0 decreases with increasing temperature T

broadening of NMR signals due to internal solid-state interactions

most important solid-state interactions:

H_{CSA} : anisotropic shielding of the magnetic field due to the anisotropic electron density in the local structure of the resonating nuclei; $\mathcal{F}$ {LP$^{(2)}$} $\Delta\nu_{CSA}$ up to 50 kHz

H_{DI} : dipolar interaction with magnetic dipole moments of neighboring spins in the local structure; $\mathcal{F}$ {LP$^{(2)}$} $\Delta\nu_{DI}$ up to 100 kHz

H_Q : quadrupolar interaction of the electric quadrupole moment of nuclei with spin I = 3/2, 5/2 etc. with electric field gradients; $\mathcal{F}$ {LP$^{(2)}$ + LP$^{(4)}$} $\Delta\nu_Q$ up to 20 MHz

Techniques of solid-state NMR spectroscopy

spin *I* = 1/2 :

magic angle spinning (MAS)

$\nu_{CSA,\ DI,\ 1QI} = \mathcal{F}\ \{(3\cos^2\Theta - 1)/2\}$

→ $\Theta = 54.7^o$

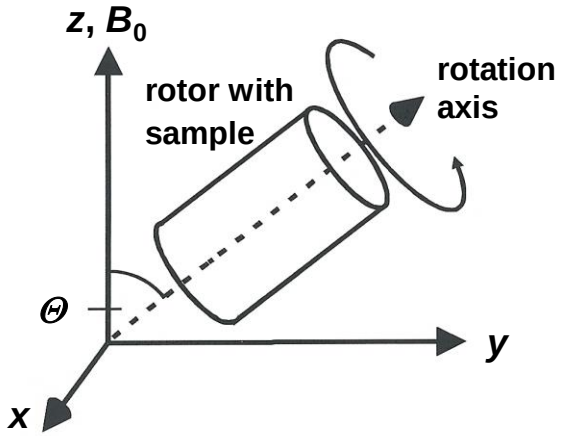

spin *I* = 3/2, 5/2 etc. :

double oriented rotation (DOR)

$\nu_{2QI} = \mathcal{F}\ \{(35\cos^4\Theta - 30\cos^2\Theta + 3)/8\}$

→ $\Theta = 30.6^o$

→ $\Theta = 70.1^o$

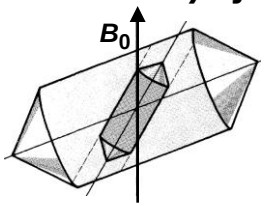

multiple-quantum MAS NMR (MQMAS)

- excitation of three- and five-quantum transitions
- recording of a spin-echo free of anisotropic contributions

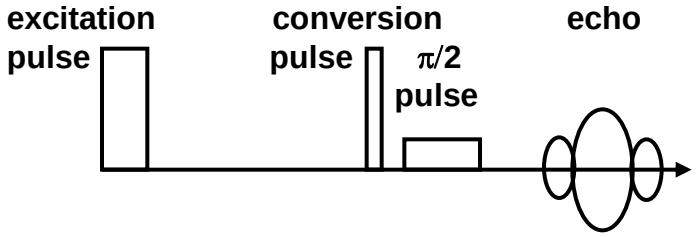

J. Amoureux et al., J. Magn. Reson A 123 (1996) 116.

Experimental techniques of *in situ* MAS NMR spectroscopy

Batch contra flow solid-state NMR experiments

batch experiments, external reaction
- **sealed samples**
- **heating in an external stove**

batch experiments, *in situ* reaction
- **sealed samples**
- **high-temperature solid-state NMR probes**
- **go-and-stop studies using a Laser heating system**

characteristics:
- **accessible with commercial equipment**
- **infinite contact time**

flow experiments, external reaction
- **reaction in an external reactor**
- **transfer of the loaded or used catalysts after quenching the reaction**

flow experiments, *in situ* reaction
- **continuous injection of reactants into the MAS NMR rotor reactor**
- **high-temperature solid-state NMR probes**

characteristics:
- **often self-made equipment**
- **study of reactions under staedy state conditions**

Preparation of catalyst samples for in situ MAS NMR studies under batch conditions

dehydration and loading of the catalyst inside the glass insert (e.g. commercial Wilmad MAS NMR inserts for 4 mm and 7 mm rotors)

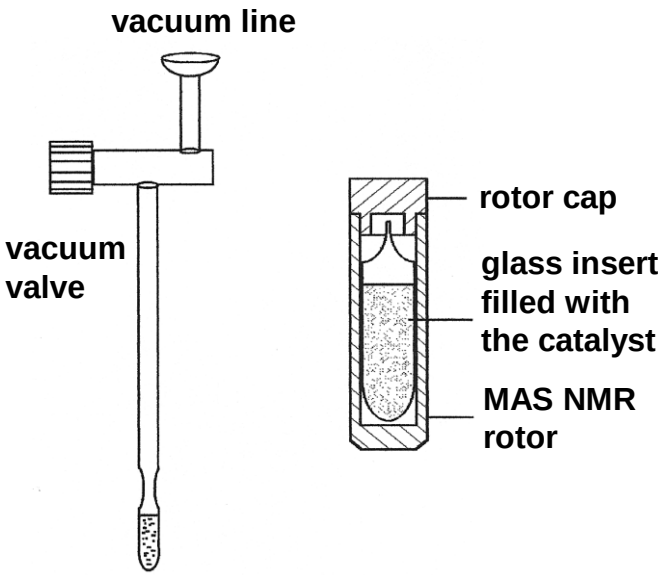

dehydration, loading, and sealing of the catalyst filled in an MAS NMR rotor inside a vacuum equipment

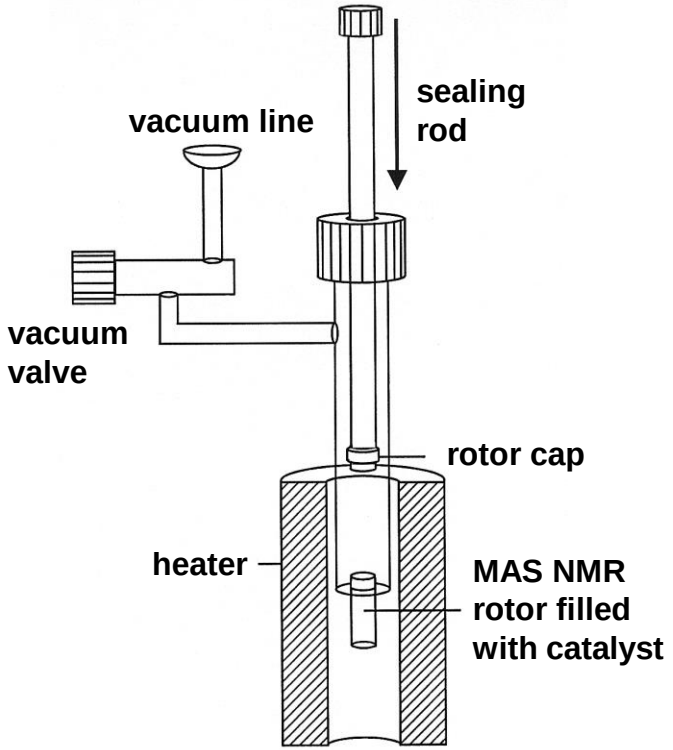

M. Hunger et al., in: B.M. Weckhuysen (ed.), *In situ Spectroscopy of Catalysts*, American Scientific Publishers, Stevenson Ranch, California, 2004, p. 177-218.

Preparation of catalyst samples for in situ MAS NMR studies under batch conditions

Wilmad insert for 7mm Bruker rotors

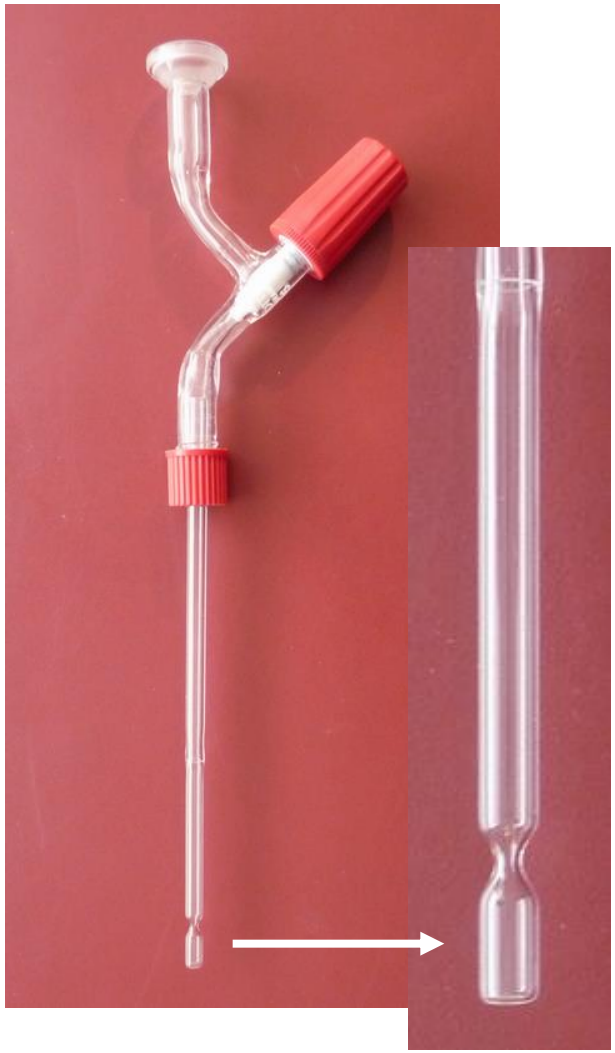

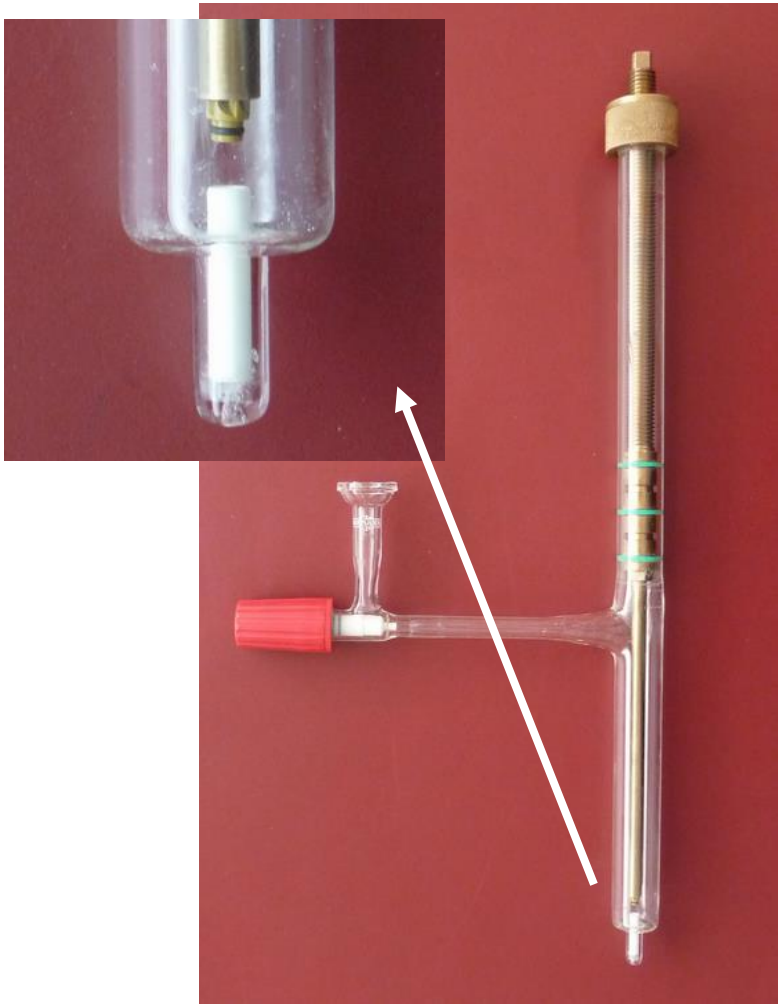

selfmade equipment for rotor sealing

Preparation of catalyst samples for in situ MAS NMR studies under batch conditions

vacuum line for dehydration of catalyst samples in glass tubes at elevated temperatures (often 673 K)

transfer of the dehydrated catalyst samples from glass tubes into MAS rotors inside a glove box (dry nitrogen)

Experimental approaches of in situ MAS NMR spectroscopy under continuous flow (CF) conditions

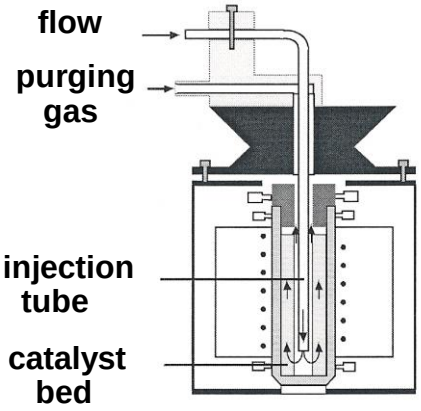

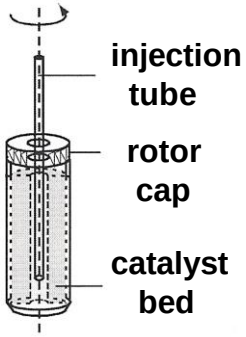

modification of Doty and Bruker MAS NMR probes with an injection system

well-defined reactant flow by using a mass-flow-controller and saturator for loading the reactants on carrier gas

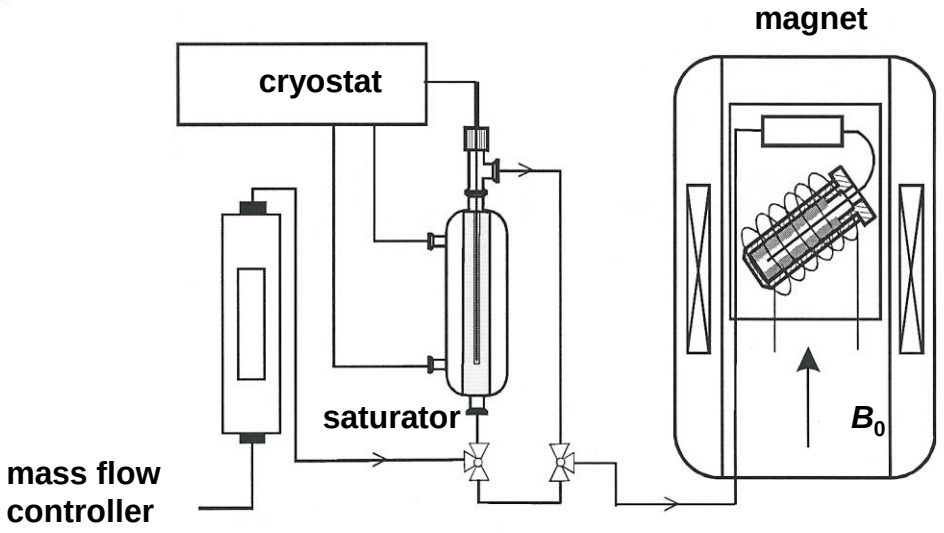

M. Hunger, T. Horvath, J. Chem. Soc., Chem. Commun. (1995) 1423.

Experimental approaches of in situ MAS NMR spectroscopy under continuous flow (CF) conditions

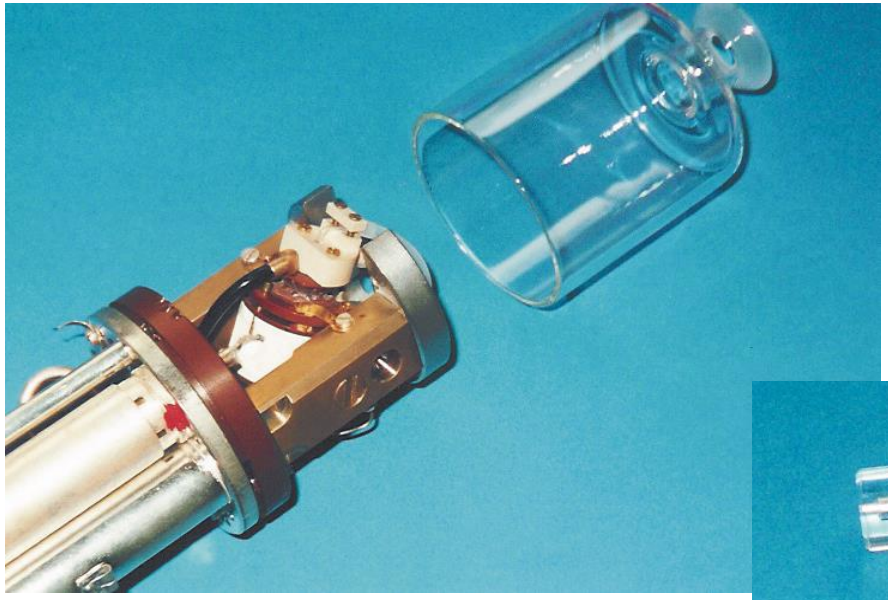

modified 4 mm Bruker MAS NMR probe equipped with an injection system

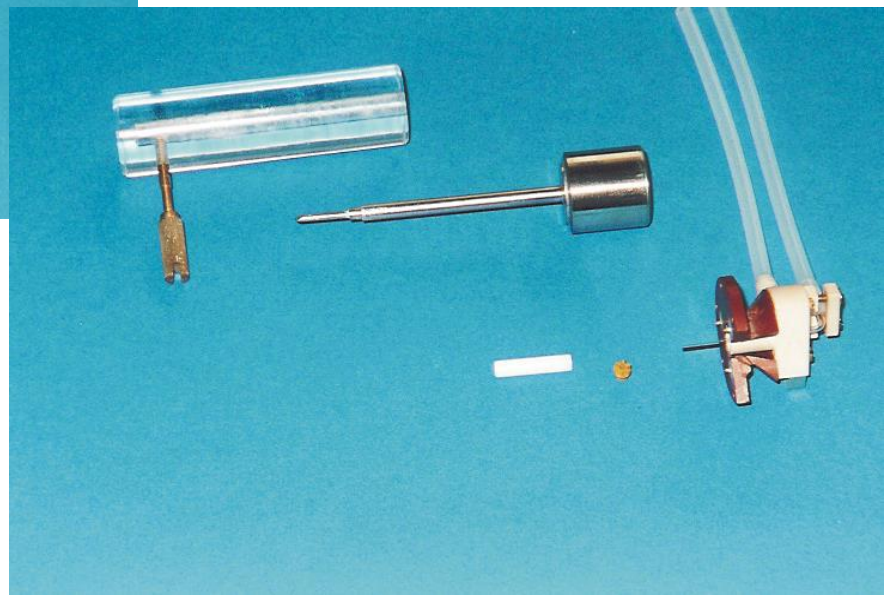

tools for shaping the catalyst to a hollow cylinder

A. Buchholz et al., Microporous & Mesoporous Mater. 57 (2003) 157.

Experimental approaches of in situ MAS NMR spectroscopy under continuous flow (CF) conditions

Bruker MASCAT probe with 7 mm MAS NMR rotor and temperatures up to 623 K

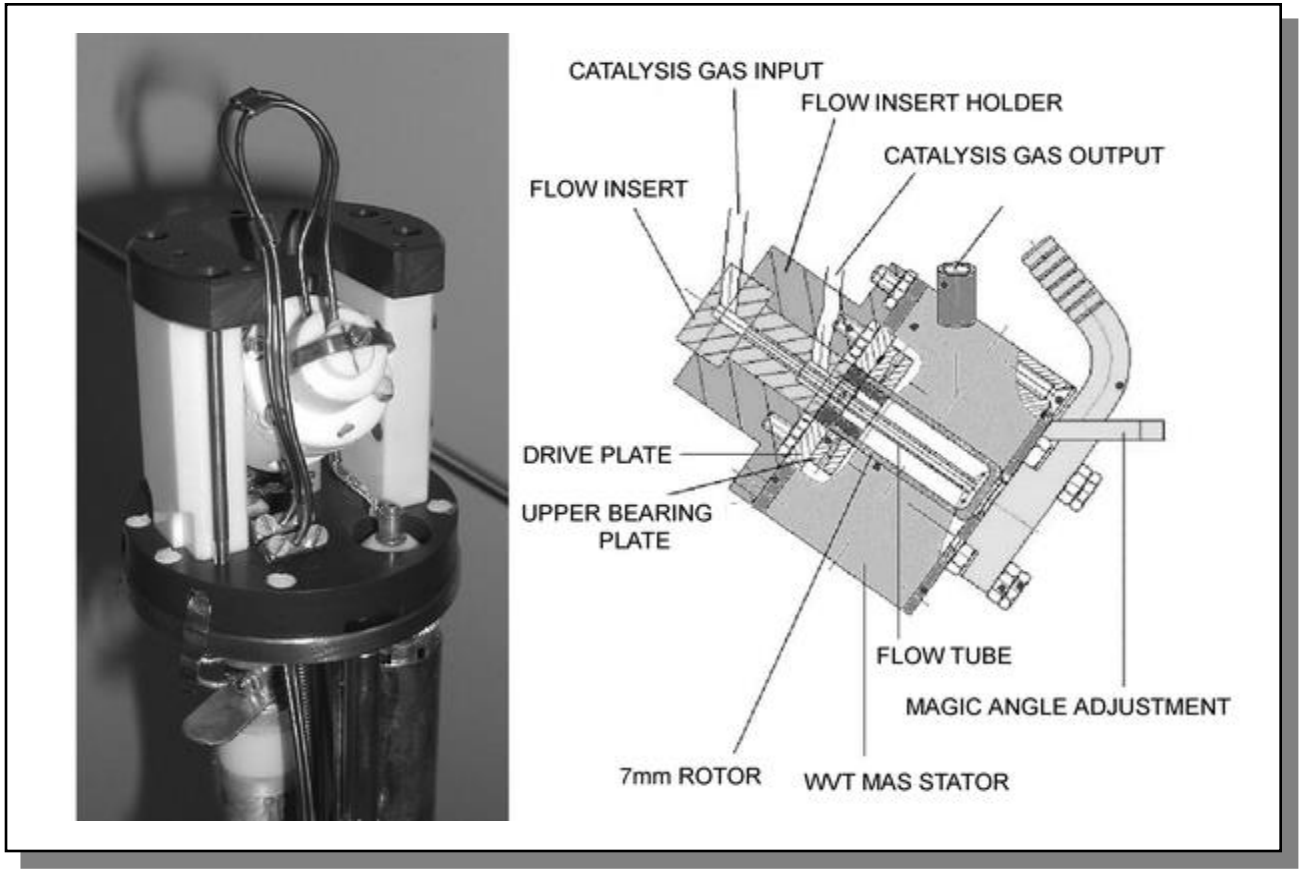

A. Nossov et al., PhysChemChemPhys. 5 (2003) 4479, and V. Sundaramurthy et al., C.R. Chimie 9 (2006) 459.

Experimental approaches of in situ MAS NMR spectroscopy under continuous flow (CF) conditions

CF MAS NMR probe with 9.5 mm rotor and for spinning rates up to 3.5 kHz at 393 K

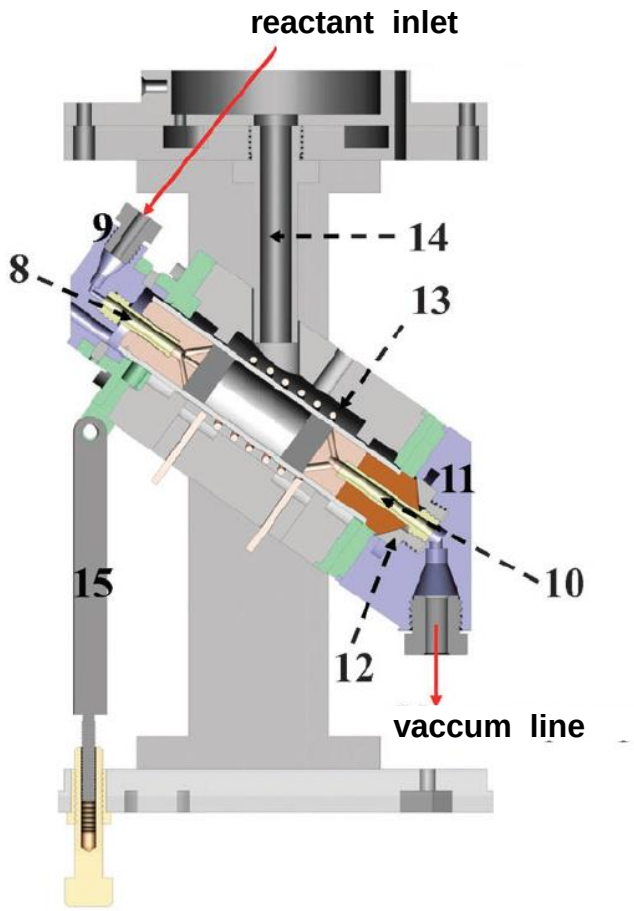

1 zirconium rotor
2 spinner tip
3 sample volume
4 glass wool spacer
5 glass wool spacer
6 end plug
7 end plug
8 injection tube
9 support block
10 exhaust tube
11 support block
12 driving jets
13 rf coil
14 heating gas inlet
15 angle adjustment

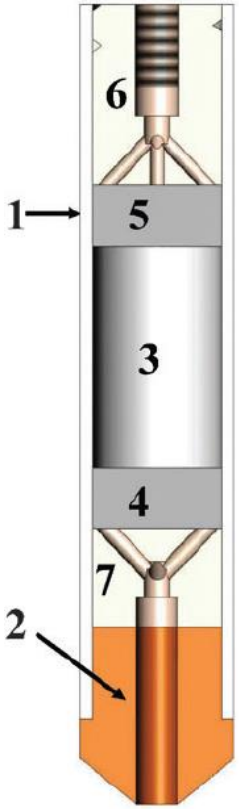

J. Z. Hu et al., PhysChemChemPhys. 14 (2012) 2137.

Coupling of in situ CF MAS NMR spectroscopy with on-line gas chromatography

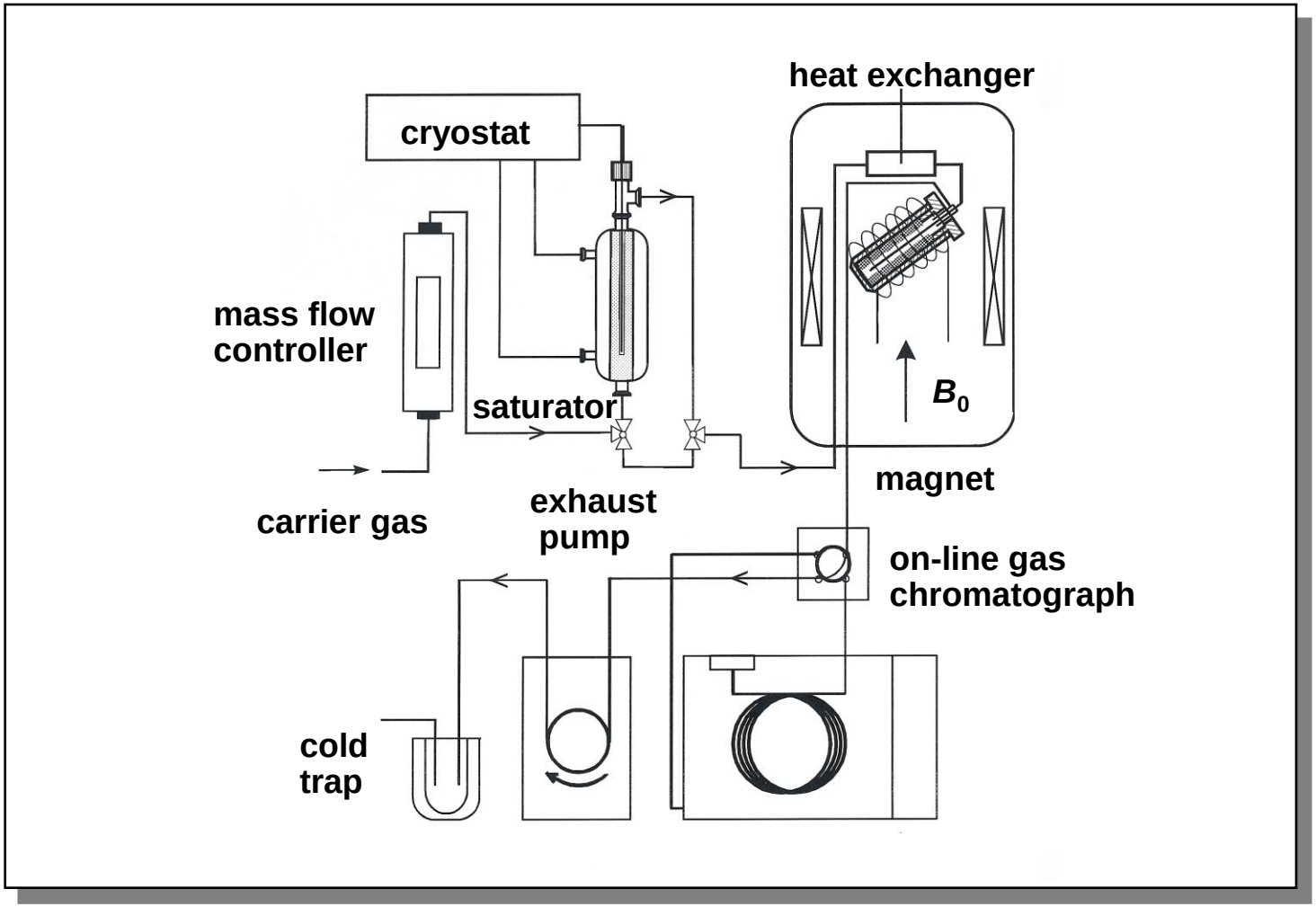

M. Hunger, Prog. Nucl. Magn. Reson. Spectrosc. 53 (2008) 105.

Coupling of in situ CF MAS NMR spectroscopy with on-line gas chromatography

methanol-to-olefin conversion on zeolite H-ZSM-5 at T = 373 to 673 K with modified residence time of W_{cat}/F_{me} = 25 gh/mol

fixed-bed reactor

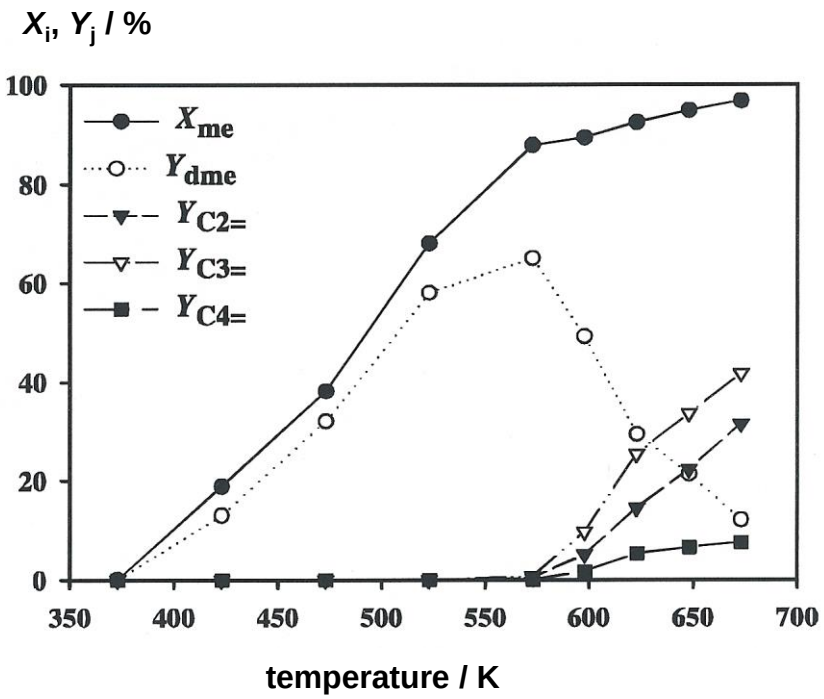

spinning (2 kHz) MAS NMR rotor reactor

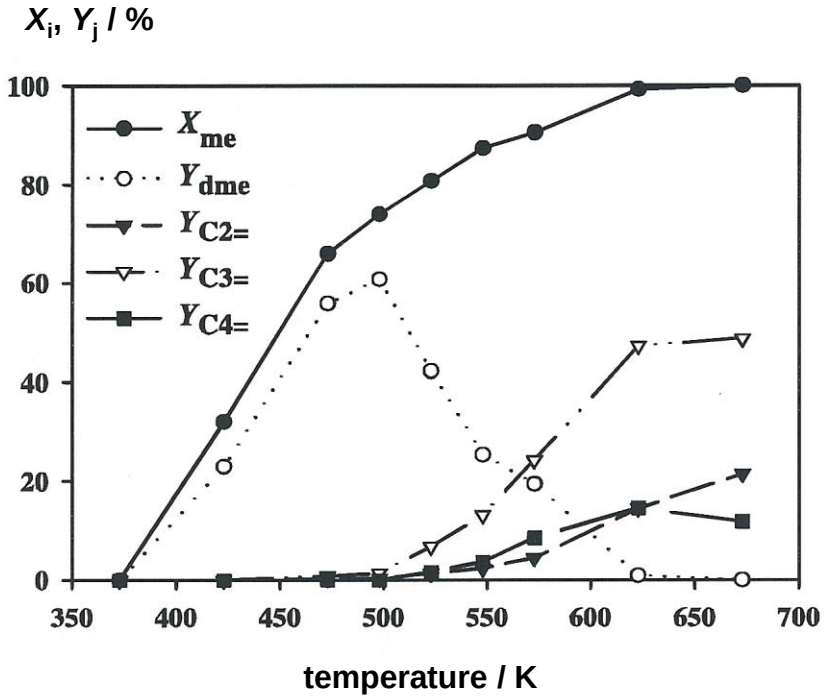

A. Buchholz, Diploma thesis, University of Stuttgart, 2001, and
M. Hunger et al., Catal. Lett. 74 (2001) 61 for SAPO-34 and SAPO-18.

Types of flow experiments for in situ MAS NMR spectroscopy

continuous-flow experiment (CF):

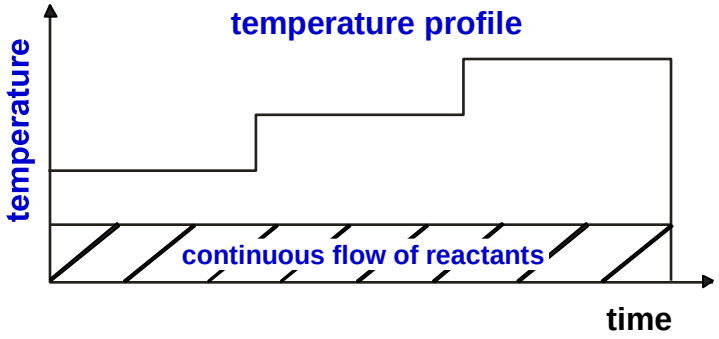

- study of adsorption or conversion of reactants at constant or different temperatures,
- study of formation of stable deposits of catalyst deactivatrion.

switched-flow experiment (SWF):

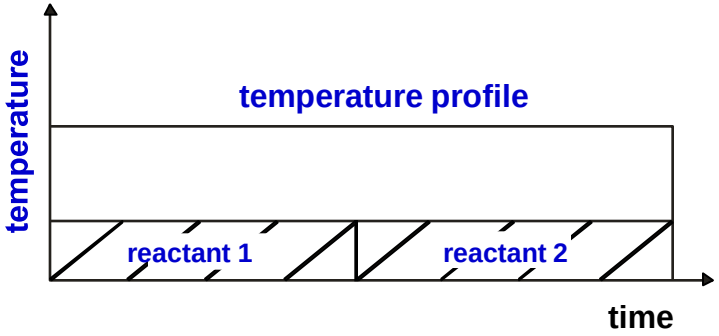

- change of isotopic enrichment in reactants,
- study of the response of the composition of reaction products or deposits on the change of reactants.

Types of flow experiments for in situ MAS NMR spectroscopy

stopped-flow experiment (SF):

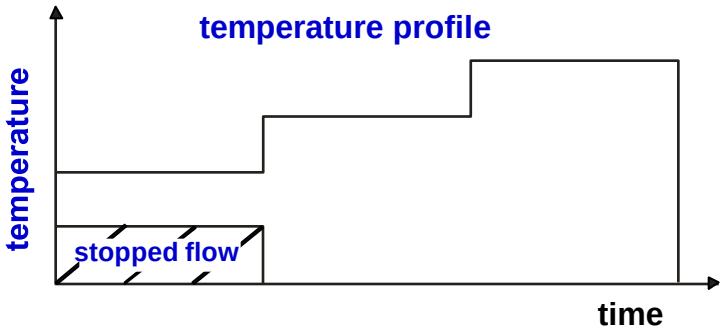

- preparation of intermediates on the catalyst,
- study of the reactivity and conversion of intermediates at constant or different temperatures.

pulsed-flow experiment (PF):

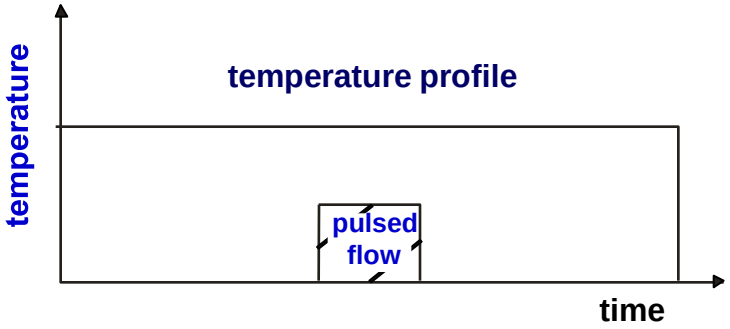

- study of the time dependence of the conversion of reactants,
- study of the isotopic exchange of reactants at high temperatures.

Experimental approach for in situ pulsed-flow MAS NMR

injection of liquid reactants into the spinning MAS NMR rotor *via* a micro-pulse pump:

pump Mikro g/5 of Fa. ProMinent, Germany, for single pulses with volumes of 2 to 50 µl

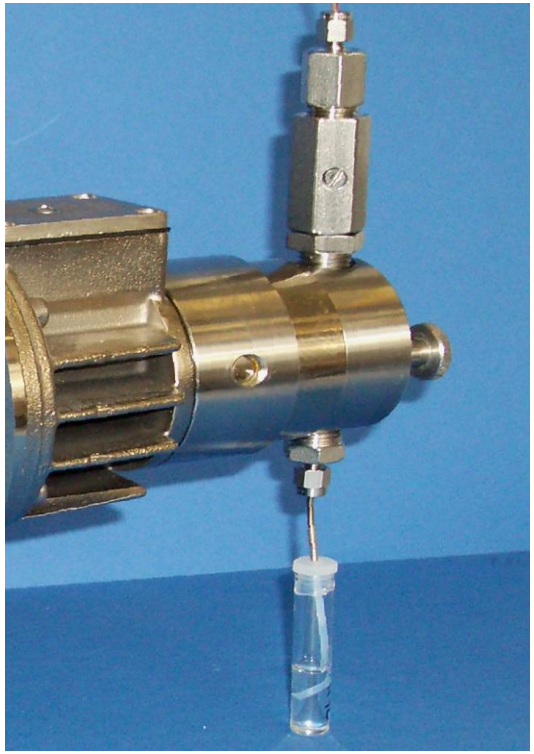

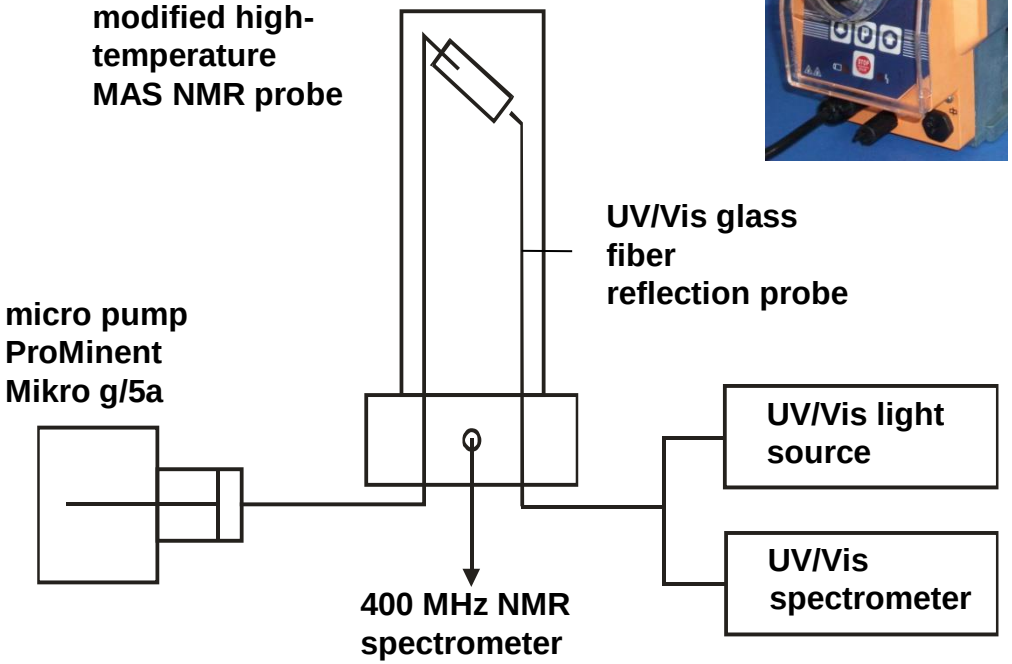

M. Hunger, Prog. Nucl. Magn. Reson. Spectrosc. 53 (2008) 105.

Coupling of in situ CF MAS NMR and UV/Vis spectroscopy via a quartz fiber at the MAS NMR stator

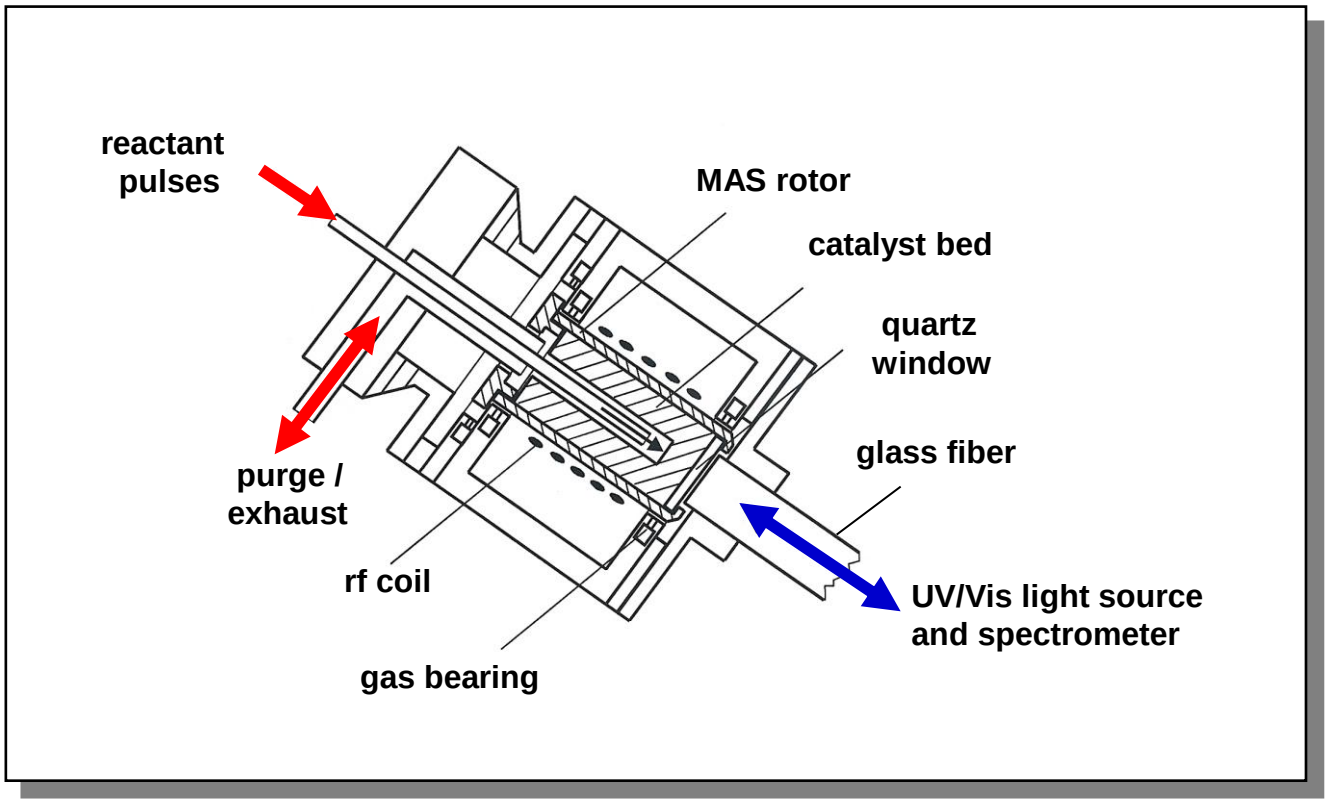

M. Hunger, Prog. Nucl. Magn. Reson. Spectrosc. 53 (2008) 105.

Coupling of in situ CF MAS NMR and UV/Vis spectroscopy via a quartz fiber at the MAS NMR stator

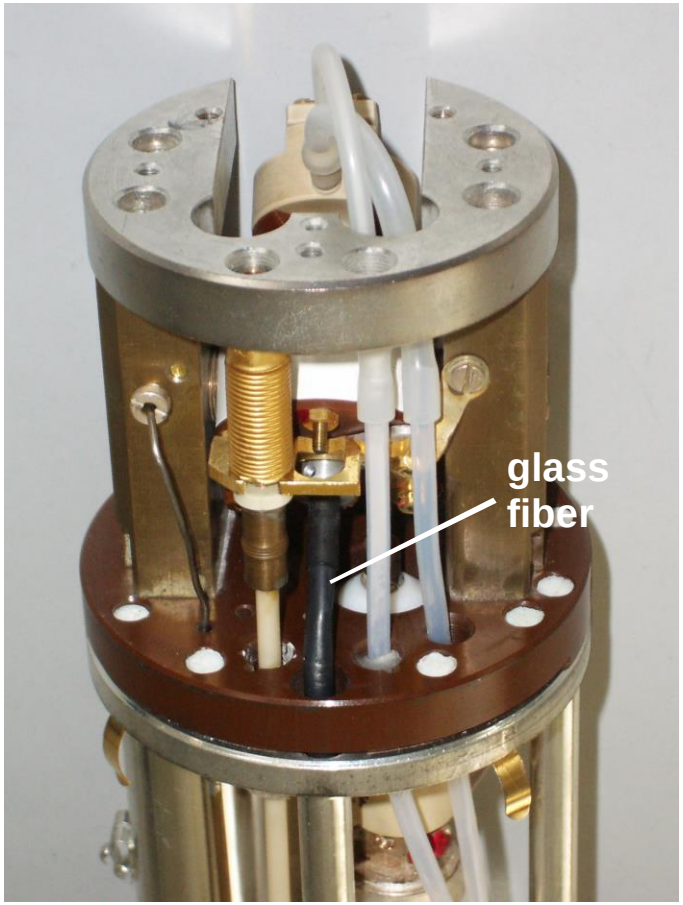

7 mm Bruker MAS NMR probe equipped with a quartz fiber (left) and UV/Vis light source and spectrometer of Avantes (bottom)

M. Hunger, Prog. Nucl. Magn. Reson. Spectrosc. 53 (2008) 105.

Examples for the application of *in situ* flow MAS NMR spectroscopy

Methanol-to-olefin (MTO) conversion on acidic zeolites

mechanism *via* olefinic compounds (H. Schulz, M. Wei, Microporous Mesoporous Mater. 29 (1999) 205)

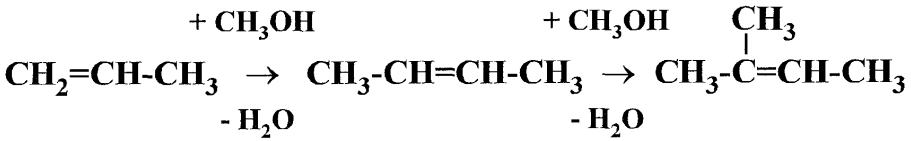

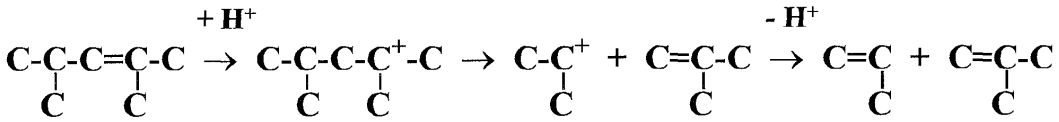

mechanism *via* polyalkylaromatics (J.F. Haw et al., Acc. Chem. Res. 36 (2003) 317)

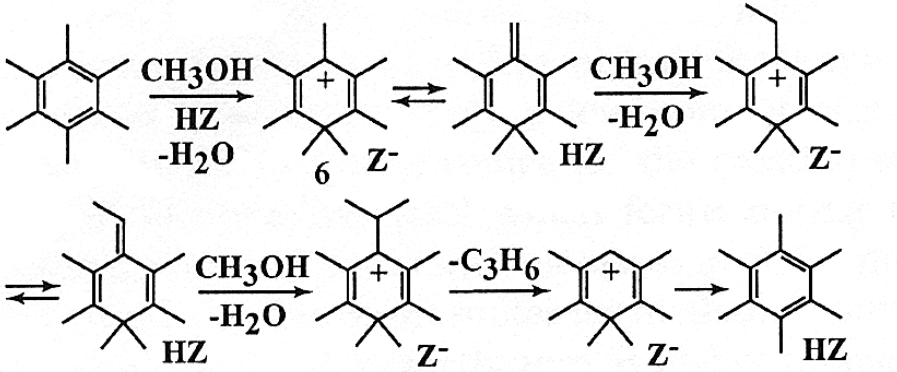

Methanol-to-olefin (MTO) conversion on acidic zeolites

H-ZSM-5: Structure type MFI

$H^+_n[Al_nSi_{96-n}O_{192}]$

crossing intersections at interconnecting 10-ring channels

[100] 0.51 nm x 0.55 nm

[010] 0.53 nm x 0.56 nm

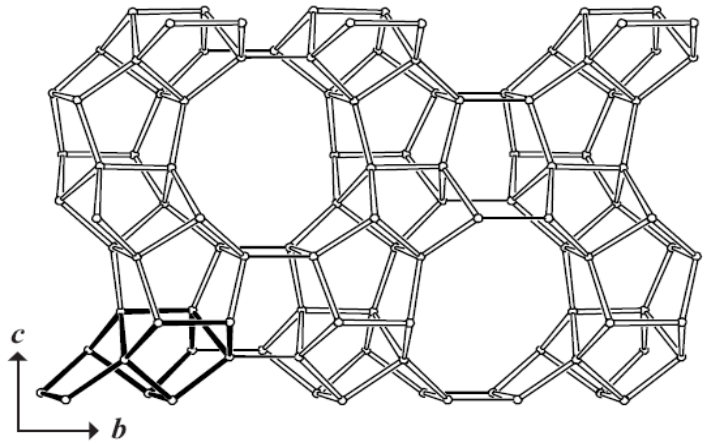

H-SAPO-34: Structure type CHA

$H^+_n[Al_{18}P_{18-n}Si_nO_{72}]$

chabazite cages accessible by 8-ring windows perpendicular to

[001] 0.38 nm x 0.38 nm

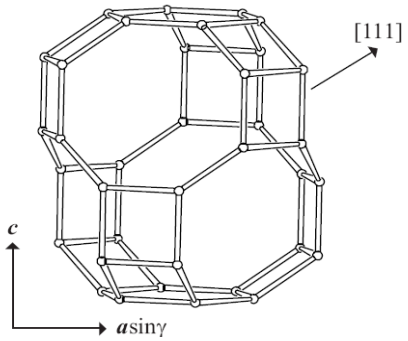

chabazite cage

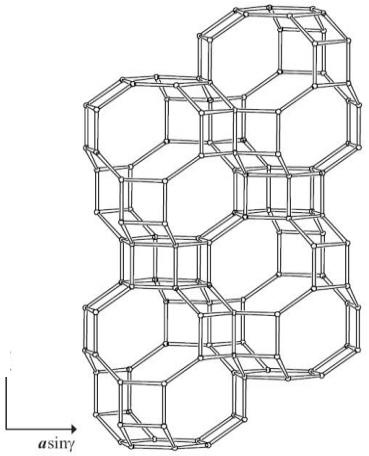

Methanol-to-olefin (MTO) conversion on acidic zeolites

in situ **^{13}C CF MAS NMR study of H-ZSM-5 (W_{cat}/F_{me} = 25 gh/mol)**

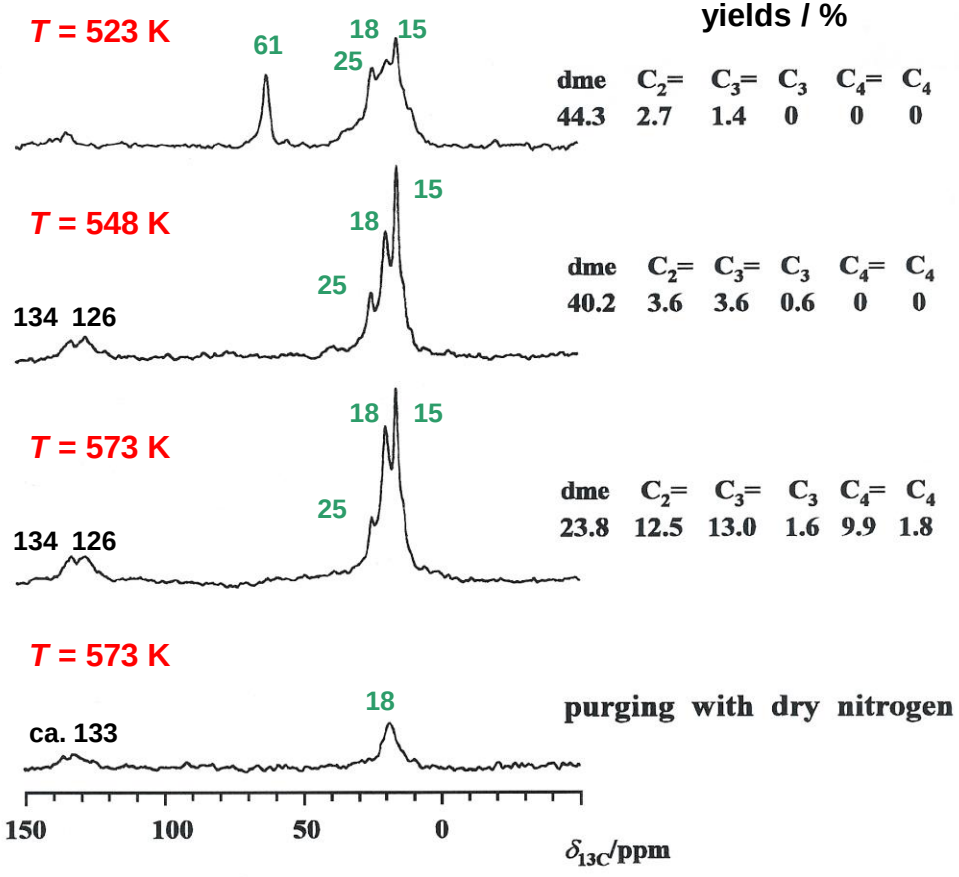

$T \lesssim 548$ K:

mixture of olefinic and aromatic compounds, such as:
- **3-hexene (14.4, 25.9, 131.2 ppm)**
- **2,4-hexadiene (17.2, 126.2, 132.5 ppm)**
- **….**
- **hexamethylbenzene (17.6, 132.1 ppm)**

T = 573 K:

polymethylaromatics remain after purging, such as:
- **toluene (20.3, 128.5, 129.0 ppm)**
- **....**
- **hexamethylbenzene (17.6, 132.1 ppm)**

M. Seiler et al., Catal. Lett. 62 (1999) 139.

Methanol-to-olefin (MTO) conversion on acidic zeolites

in situ **^{13}C CF MAS NMR study of H-SAPO-34 (W_{cat}/F_{me} = 25 gh/mol)**

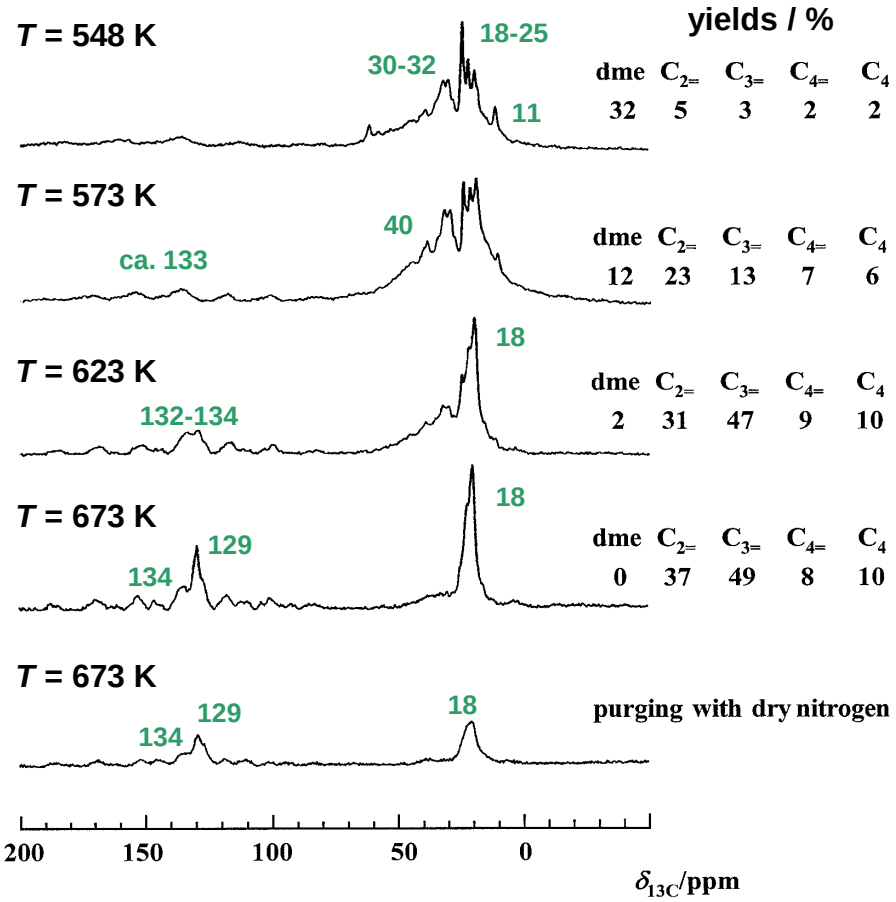

$T \lesssim 573$ K:

mixture of olefinic and aromatic compounds, such as:

2-methyl-2-butene (9.3-22.5, 118.8, 131.8 ppm)
2,4-hexadiene (19.5, 132.5 ppm)
….
tetramethylbenzene (18.9, 131.1, 134.0 ppm)

$T > 573$ K:

domination of polymethyl-aromatics, such as:

toluene (20.3, 128.5, 129.0 ppm)
….

trimethylbenzene (21.2, 127.4, 137.6 ppm)
hexamethylbenzene (17.6, 132.1 ppm)

M. Hunger et al., Catal. Lett. 74 (2001) 61.

Methanol-to-olefin (MTO) conversion on acidic zeolites

in situ **^{13}C SWF MAS NMR study of MTO on H-ZSM-5 at T = 573 (W_{cat}/F_{me} = 25 gh/mol)**

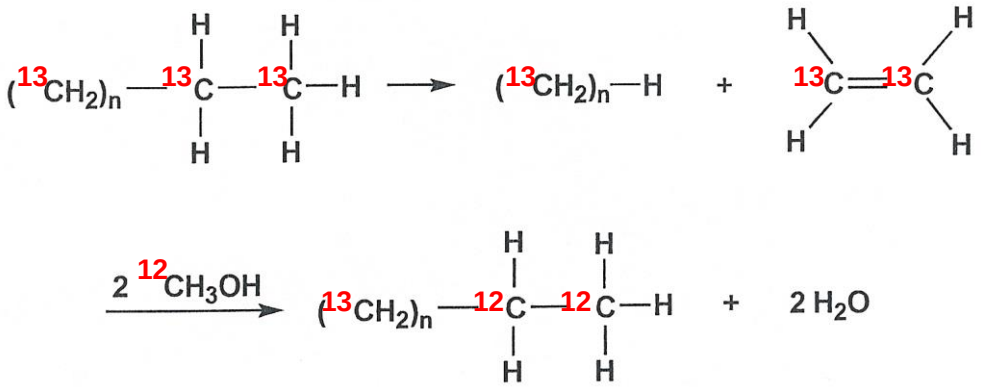

^{13}C SWF MAS NMR **^{1}H SWF MAS NMR**

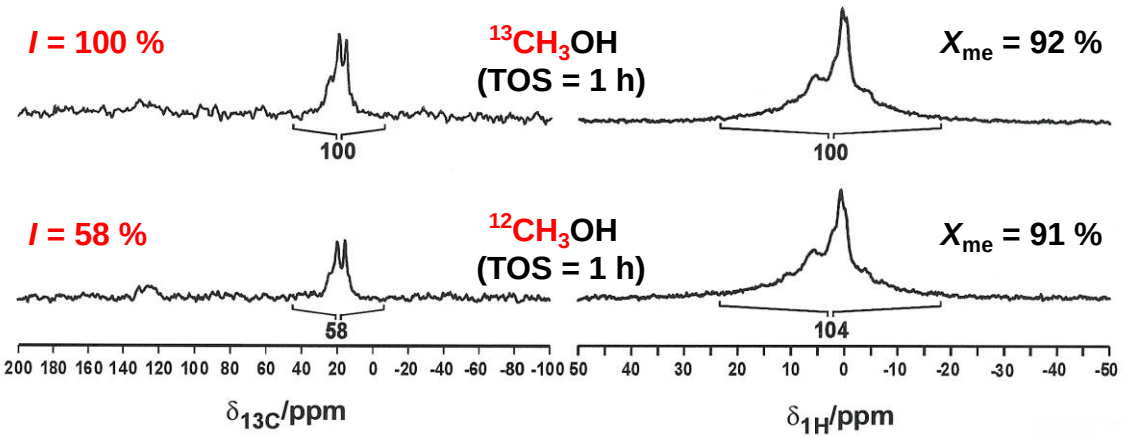

switching of the reactant flow induces a decrease of the ^{13}C-isotopes in the organic deposits:

- **alkyl groups are involved in the formation of olefins**
- **carbon pool plays an active role in the MTO process**

M. Seiler et al., Catal. Lett. 88 (2003) 187.

Methanol-to-olefin (MTO) conversion on acidic zeolites

in situ **^{13}C CF MAS NMR-UV/Vis study of coke formation on H-SAPO-34 during the MTO conversion with W_{cat}/F_{me} = 25 gh/mol**

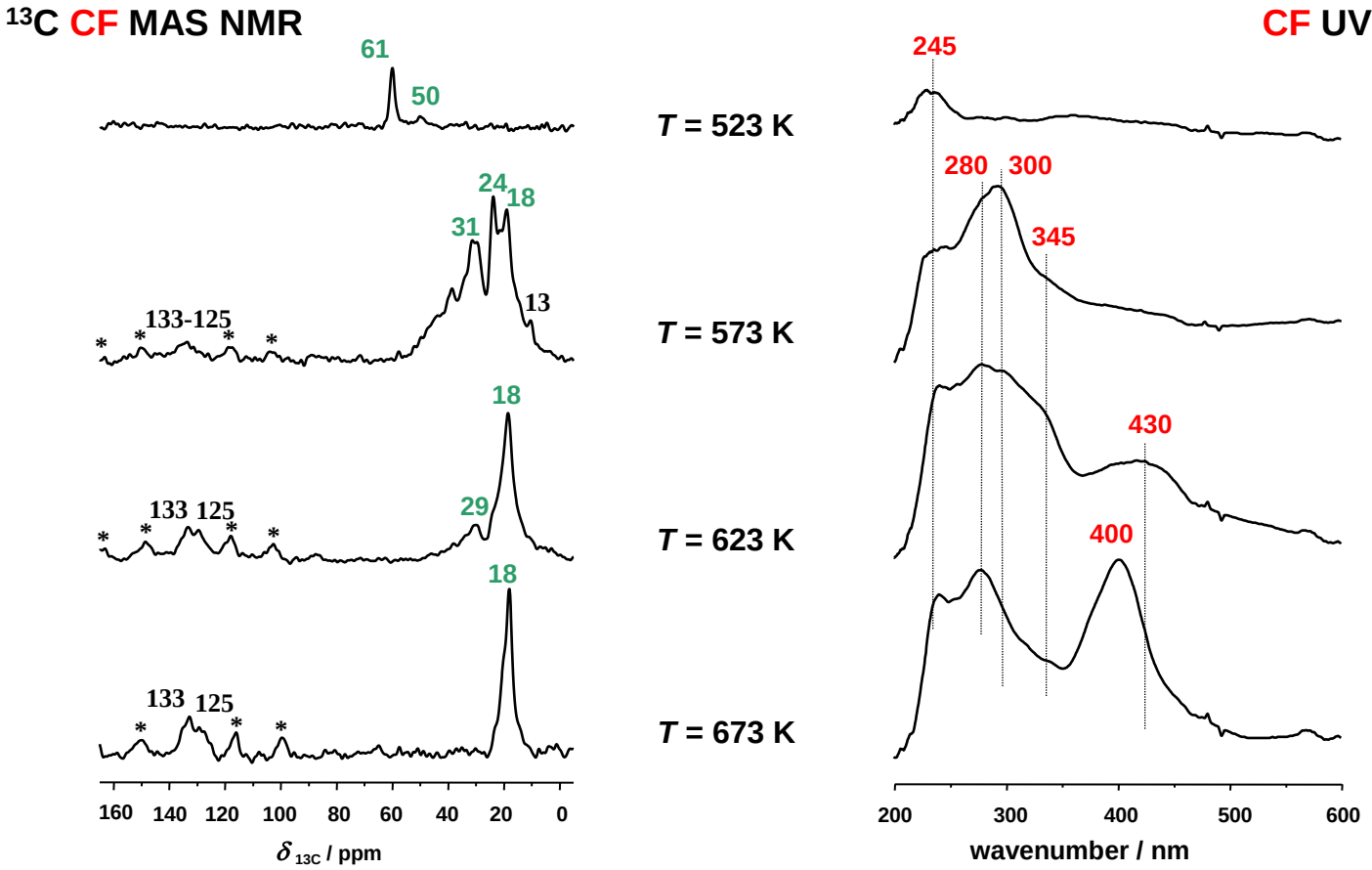

245 nm: dienes
280 nm: polyalkylaromatics
300 nm: monoenylic carbenium
345 nm: dienylic carbenium
400 nm: polycyclic coke
430 nm: trienylic carbenium

Y. Jiang et al., Microporous Mesoporous Mater. 105 (2007) 132.

Side-chain H/D exchange of ethylbenzene on steamed zeolite deH,Na-Y/81.5

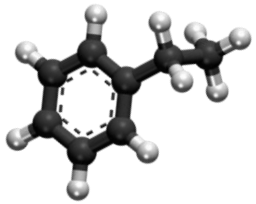

$C_6H_5CD_2CD_3$ + SiOHAl ⟶ $C_6H_5CDHCD_2H$ + SiODAl

7.3 3.8 deH,Na-Y/81.5 2.7 1.2 ppm

^{1}H NMR shift values

***in situ* ^{1}H PF MAS NMR experiments:**

- pulses of 7.8 mg ethyl-d_5-benzene,
- 32 scans per spectrum with repetition time of 10 s at 9.4 T,
- sample spinning rate of *ca.* 2 kHz.

message:

- regioselective H/D exchange at 443 to 463 K (^{1}H MAS NMR),
- different types of carbenium ions (UV/Vis)-

^{1}H PF MAS NMR

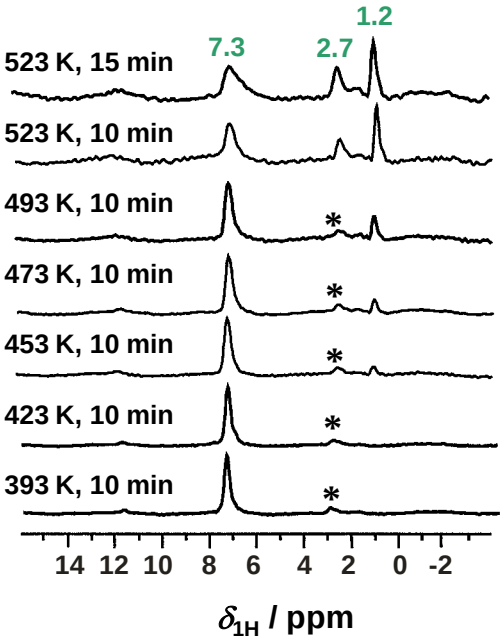

PF UV/Vis

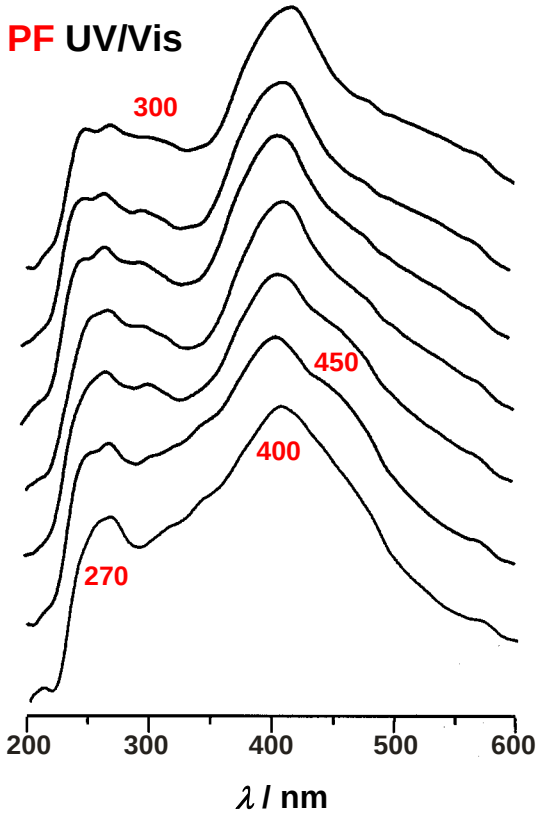

J. Huang et al., ChemPhysChem 9 (2008) 1107.

Side-chain H/D exchange of ethylbenzene on steamed zeolite deH,Na-Y/81.5

$C_6H_5CD_2CD_3$ on dealuminated zeolite deH,Na-Y/81.5 (24.5 Al^{ex}/u.c., 10.9 SiOHAl /u.c.)

***in situ* ^{1}H PF MAS NMR**

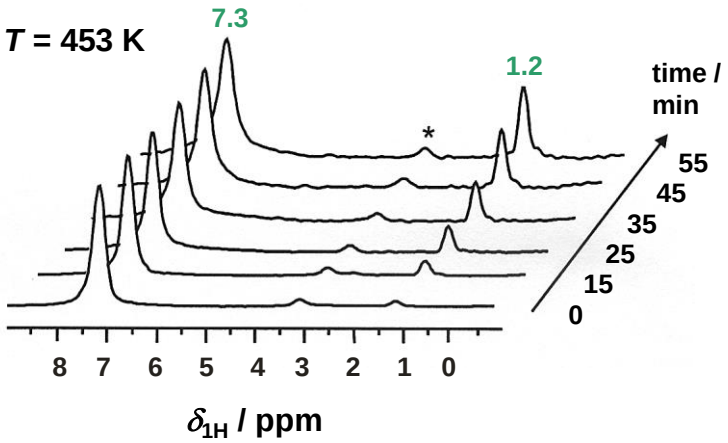

Arrhenius plot

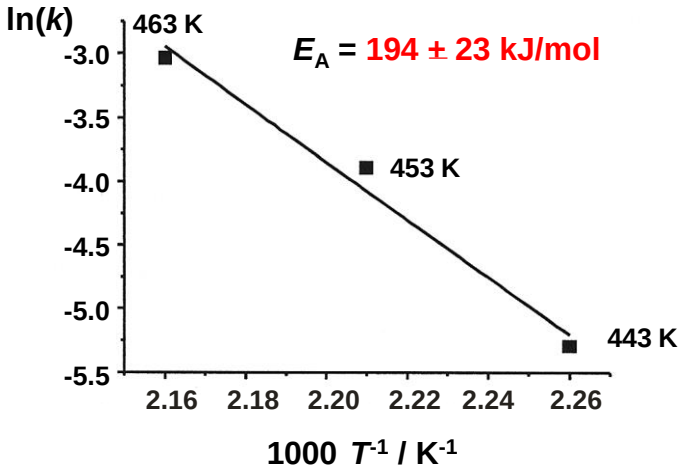

activation energy of the regioselective H/D exchange (E_A = 194 kJ/mol) indicates that a hydride transfer reaction is the rate determining step

J. Huang et al., ChemPhysChem 9 (2008) 1107.

Side-chain H/D exchange of ethylbenzene on steamed zeolite deH,Na-Y/81.5

^{1}H PF MAS NMR:

- selective H/D exchange of methyl groups (1.2 ppm),
- activation energy of 194 kJ/mol indicates hydride transfer.

PF UV/Vis:

- ethylcyclohexadienyl carbenium ions at BAS (400 nm), A,
- sec-ethylphenyl carbenium ions at LAS (450 nm), B,
- styrene at BAS (300 nm), C.

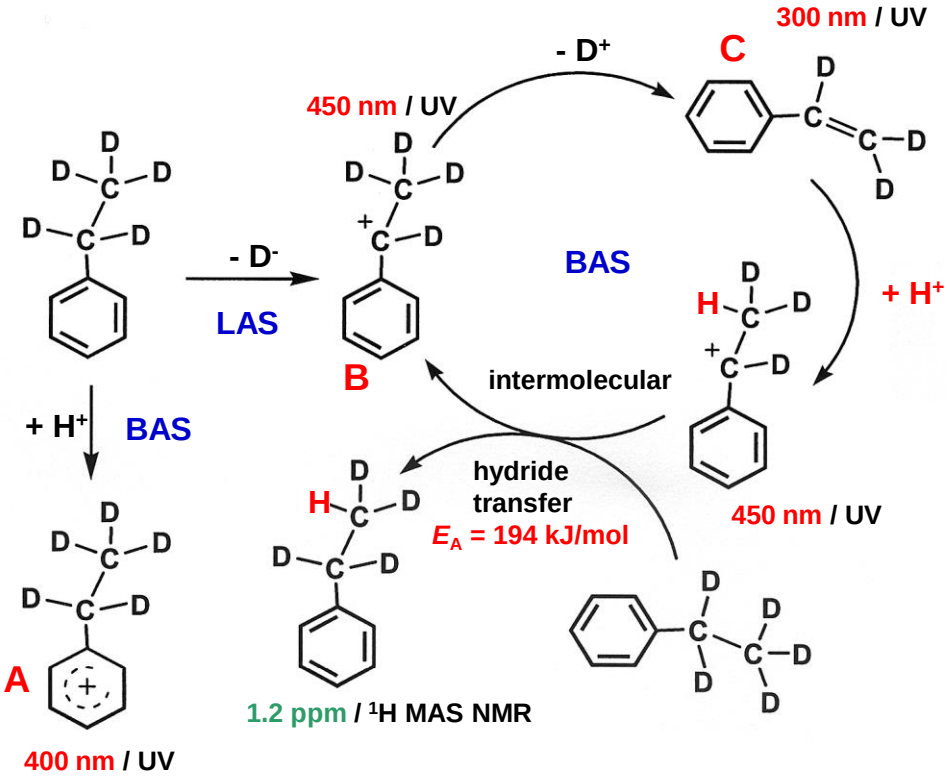

BAS: Broensted acid sites LAS: Lewis acid sites

J. Huang et al., ChemPhysChem 9 (2008) 1107.

Study of the intrinsic of the hydrogenation rate of acrylonitrile on Pt- and Rh-containing zeolites Y

hydrogenation of pre-adsorbed acrylonitrile with normal H_2 at T = 295 K

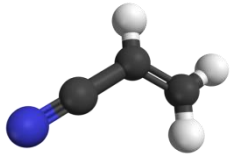

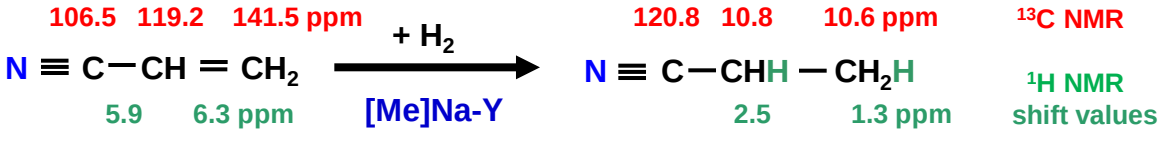

in situ ^{1}H CF MAS NMR of acrylonitrile hydrogenation on 0.9[Pt]Na-Y

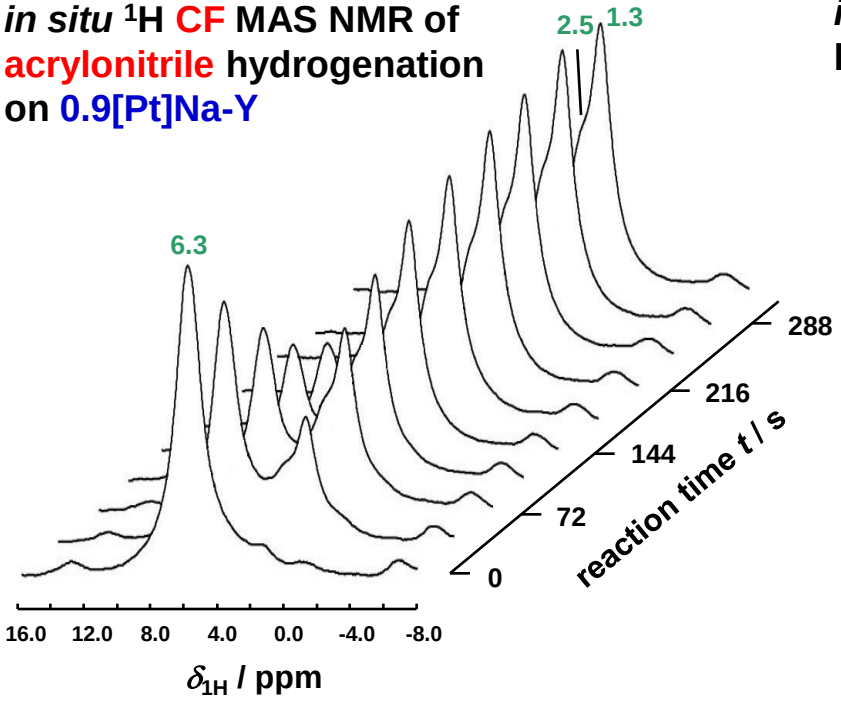

in situ ^{13}C CF MAS NMR of acrylonitrile hydrogenation on 0.9[Pt]Na-Y

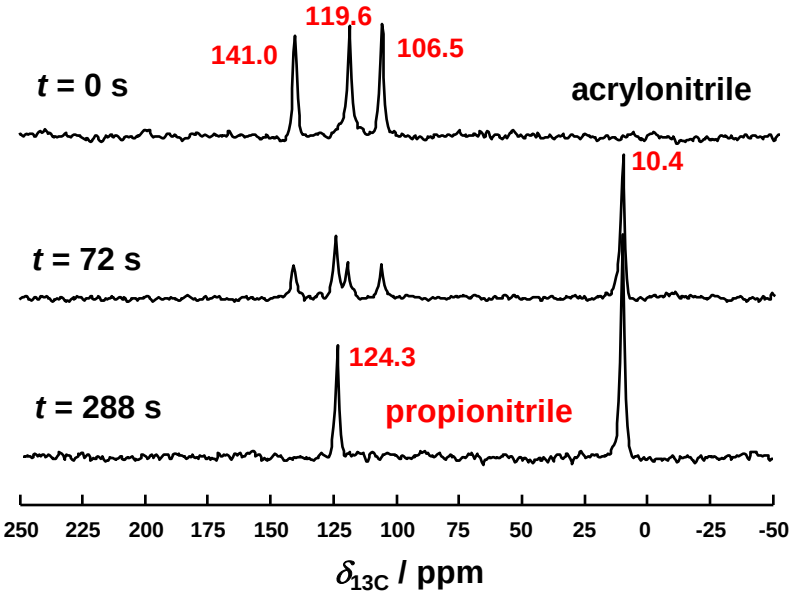

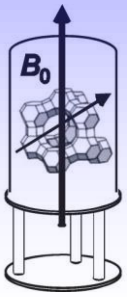

Bruker Avance III 400WB spectrometer, modified 7 mm MAS NMR probe, ν_{rot} ca. 2 kHz, 1 FID / ^{1}H NMR spectrum, D1 = 6 s.

H. Henning et al., Micropor. Mesopor. Mater. 164 (2012) 104.

Study of the intrinsic of the hydrogenation rate of acrylonitrile on Pt- and Rh-containing zeolites Y

in situ ^{1}H CF MAS NMR of acrylonitrile hydrogenation on 0.4[Rh]Na-Y

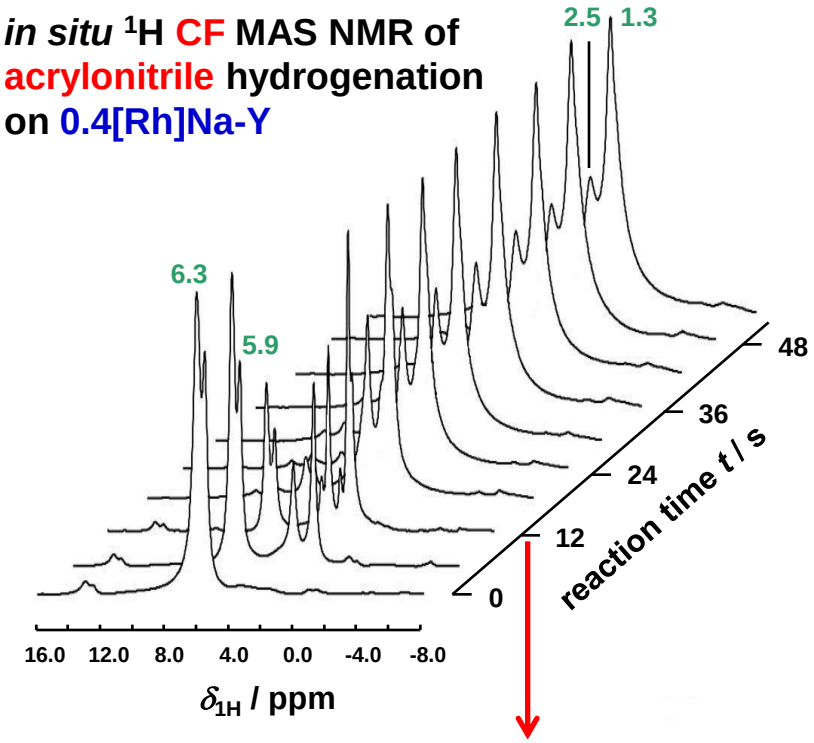

*: formation of half-hydrogenated intermediates?

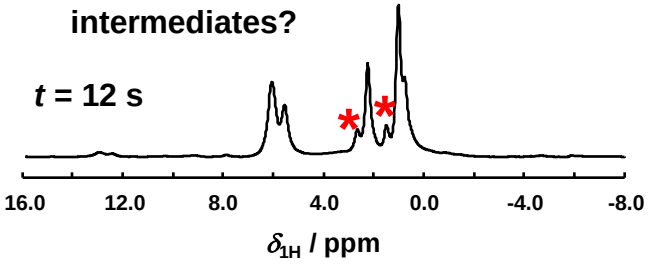

comparison of the intrinsic hydrogenation rates

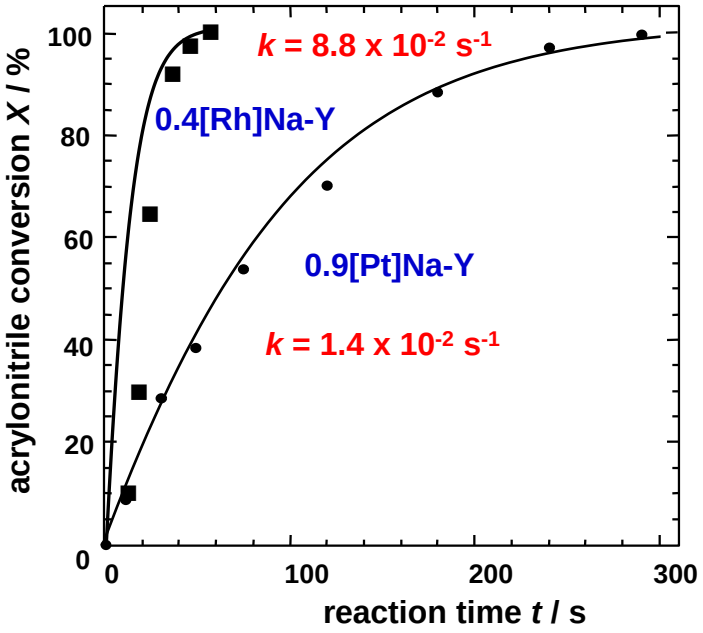

Rh atoms cause a factor 6 higher intrinsic hydrogenation rate compared with Pt atoms dispersed on zeolite Na-Y

H. Henning et al., Micropor. Mesopor. Mater. 164 (2012) 104.

Hyperpolarization experiments utilizing *in situ* CF MAS NMR techniques

CF MAS NMR experiments with Laser-polarized ^{129}Xe

continuous injection of Laser-polarized xenon:

- optical pumping of the D1 transition of rubidium,

- spin exchange between excited rubidium atoms and xenon atoms by gas phase collisions.

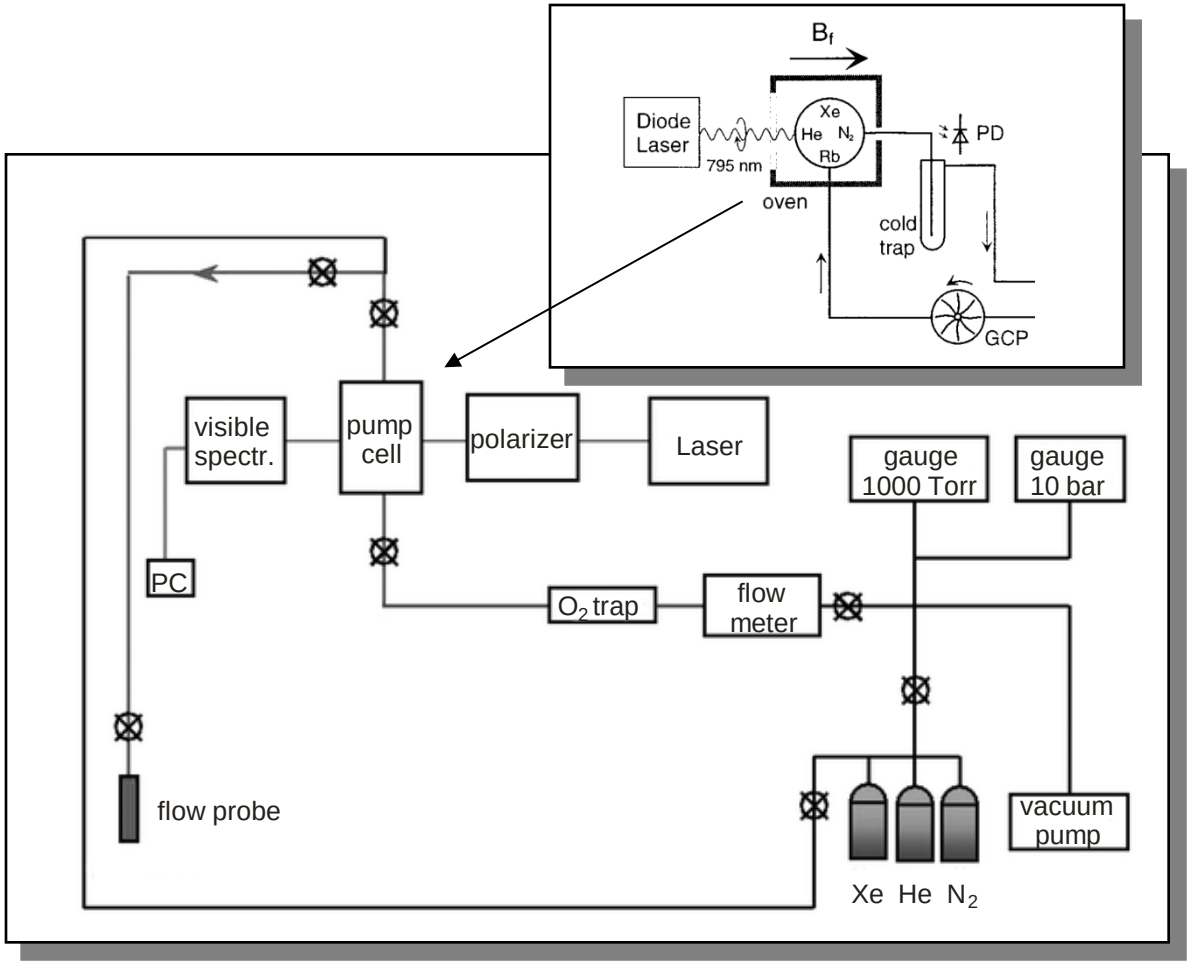

typical applications:

- study of the meso- and micropore systems of solid catalyst and adsorbents,

- study of the location of adsorbate complexes upon *in situ* adsorption of reactants.

M. Haake et al., J. Am. Chem. Soc. 119 (1997) 11711, and
A. Nossov et al., Phys. Chem. Chem. Phys. 5 (2003) 4479.

CF MAS NMR experiments with Laser-polarized ^{129}Xe

solid-state ^{129}Xe CF NMR study of Laser-polarized xenon adsorbed on ITQ-6 (layered precursor of zeolite ferrierite):

- **helium flow of 100 cm^3 min^{-1} with 1 % hyperpolarized xenon,**
- **magnetic field of 7.0 T,**
- **sufficient resolution requires application of MAS,**
- **1000 scans with repetition time of 1 s (16.7 min).**

signal assignment:

- **signal at 65 ppm is xenon in the interlamellar space,**
- **signal at 100 ppm is xenon in cavities,**
- **signal at 135 ppm corresponds to xenon in micropores (e.g. 8- or 10-ring pores of FER domains).**

solid-state ^{129}Xe CF NMR of ITQ-6

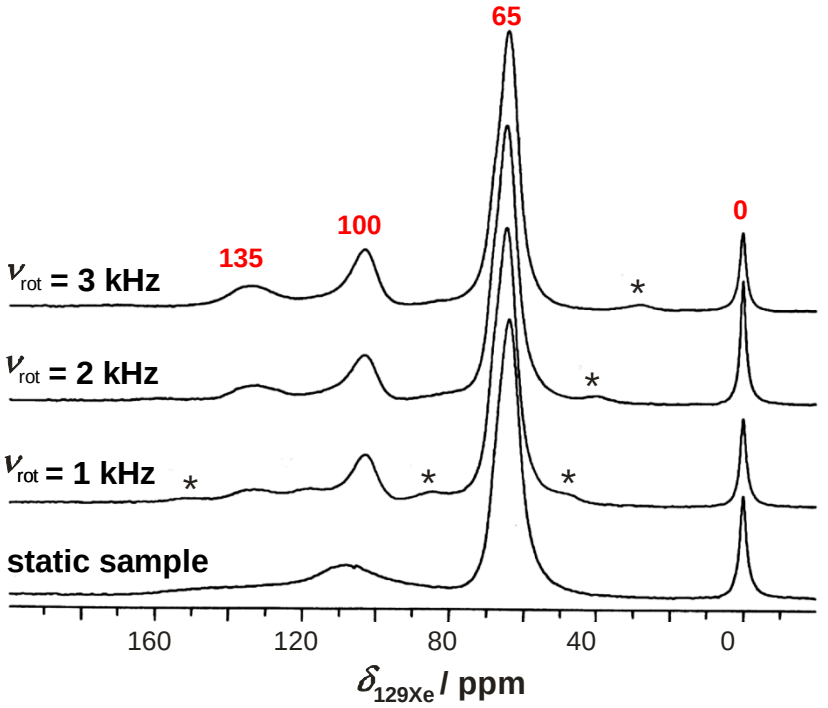

A. Nossov et al., Phys. Chem. Chem. Phys. 5 (2003) 4479.

CF MAS NMR experiments with Laser-polarized ^{129}Xe

2D-exchange ^{129}Xe CF MAS NMR of Laser-polarized ^{129}Xe adsorbed on ITQ-6:

- **helium flow of 100 cm^3 min^{-1} with 1 % hyperpolarized ^{129}Xe,**
- **magnetic field of 7.0 T,**
- **ν_{rot} = 3 kHz and mixing time of 50 ms,**
- **8 scans with repetition time of 2 s and 256 increments (68 min).**

cross peaks indicate ^{129}Xe exchange between:

a) gas phase and the interlamellar space,

b) interlamellar space and cavities,

c) cavities and micropores.

2D-exchange ^{129}Xe CF MAS NMR of ITQ-6

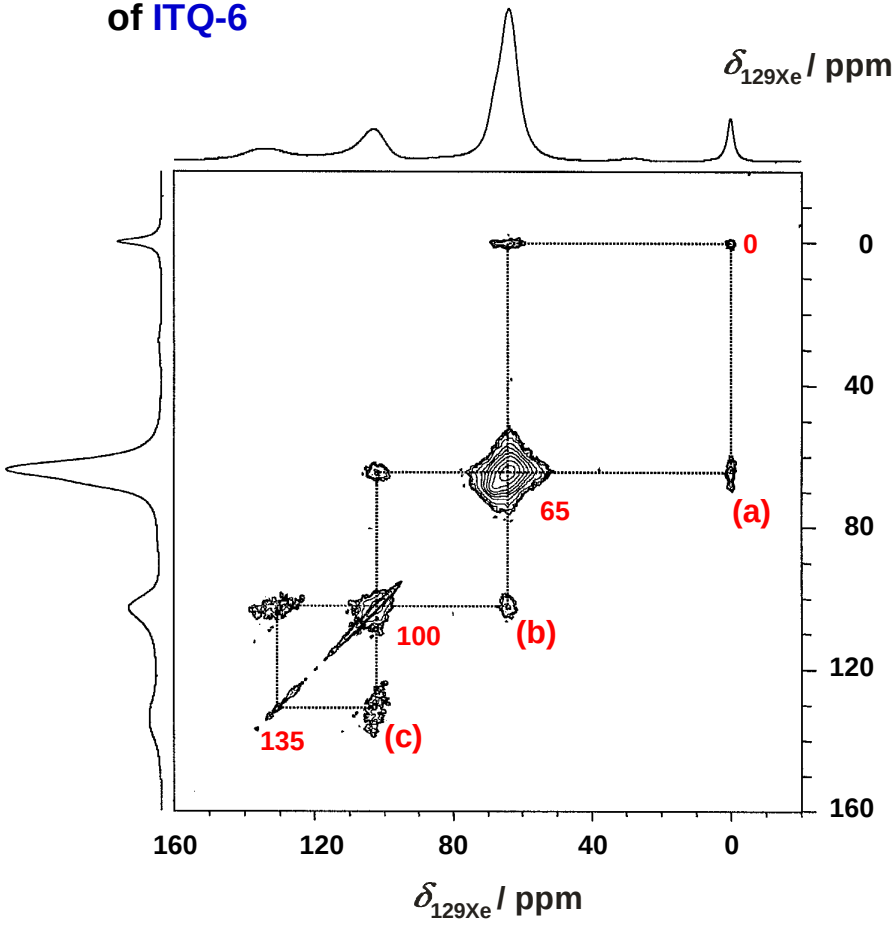

A. Nossov et al., Phys. Chem. Chem. Phys. 5 (2003) 4479.

CF MAS NMR experiments with Laser-polarized ^{129}Xe

^{129}Xe CF MAS NMR of Laser-polarized xenon on silicalite-1:

- helium flow with 1 % hyperpolarized xenon,
- magnetic field of 7.0 T,
- ν_{rot} = 3.5 kHz,
- signal at 103 ppm caused by xenon in empty 10-ring channels.

pulsed addition of benzene (1.3 %):

- resonance shift to left due to adsorption of benzene in 10-ring channels (b, d, f),
- resonance shift to right due to desorption of benzene, i.e, 1.5 h later (c, e).

^{129}Xe CF MAS NMR upon ad-/desorption of benzene on silicalite-1

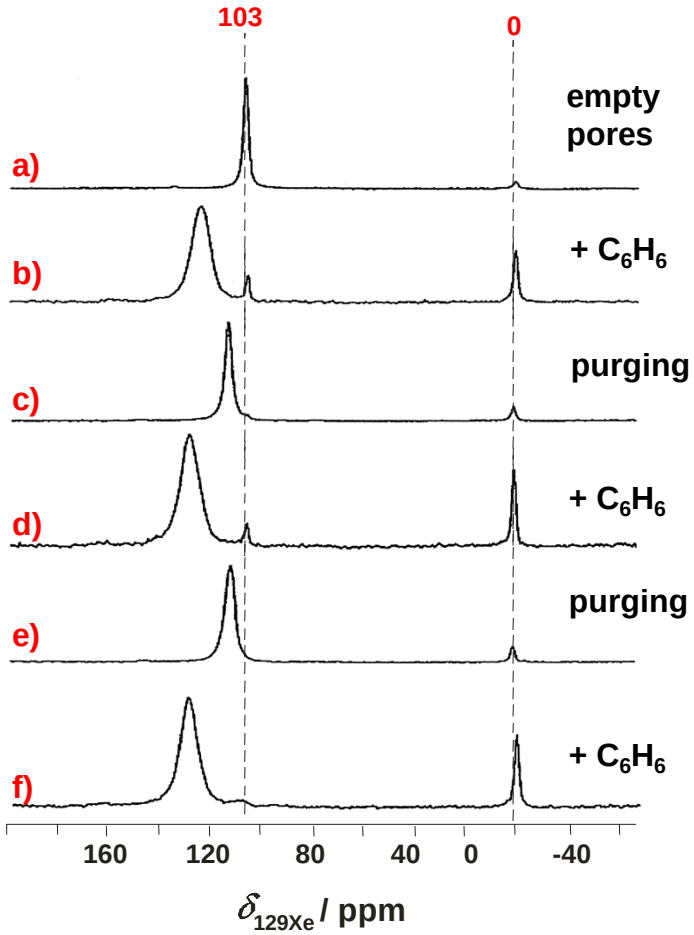

I.L. Moudrakovski et al., Chem. Mater. 12 (2000) 1181

.

CF MAS NMR of parahydrogen-induced polarization (PHIP)

PASADENA: Parahydrogen And Synthesis Allow Dramatically Enhanced Nuclear Alignment (p-H_2 incorporation inside the B_0 field)

hydrogenation of propene with para-enriched H_2 **p-H_2:**

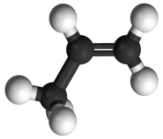

$$CH_3-CH=CH_2 \xrightarrow{+\ p\text{-}H_2} CH_3-CHH-CH_2H$$

- **pairwise incorporation of the two H atoms of a p-H_2 causes a large non-equilibrium spin polarization**

- **^{1}H MAS NMR signals due to a pairwise incorporation of p-H_2 into reactants have typical antiphases (see Figure)**

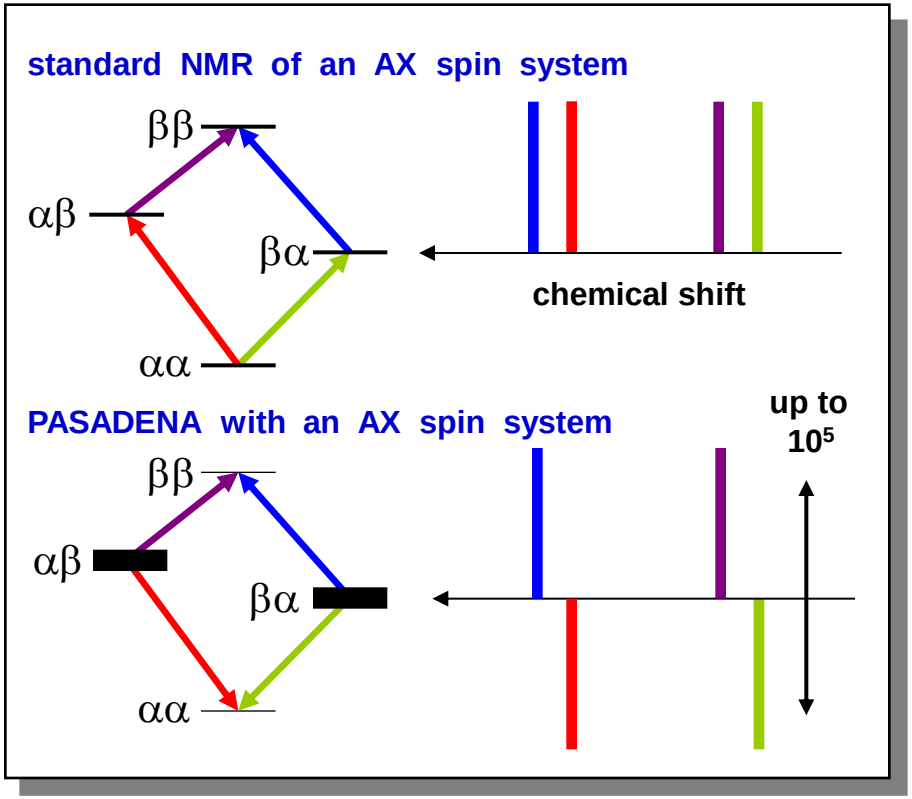

J. Natterer, J. Bargon, Prog. Nucl. Magn. Reson. Spec. 31 (1997) 293.

CF MAS NMR of parahydrogen-induced polarization (PHIP)

PASADENA: Parahydrogen And Synthesis Allow Dramatically Enhanced Nuclear Alignment (p-H_2 incorporation inside the B_0 field)

Equipment for *in situ* ^{1}H CF MAS NMR studies of PHIP:

- **at ν_0 = 400.13 MHz, ν_{rot} = 3 kHz, $\pi/4$ pulses, NS = 96, D1 = 0.1 s,**
- **modified Bruker 7 mm MAS NMR probe,**
- **para : ortho ratio of 1 : 1 using a tube filled with FeO(OH) (Sigma-Aldrich) placed in liquid nitrogen,**
- **hydrogen and propene flows of 25 ml/min (1 : 1).**

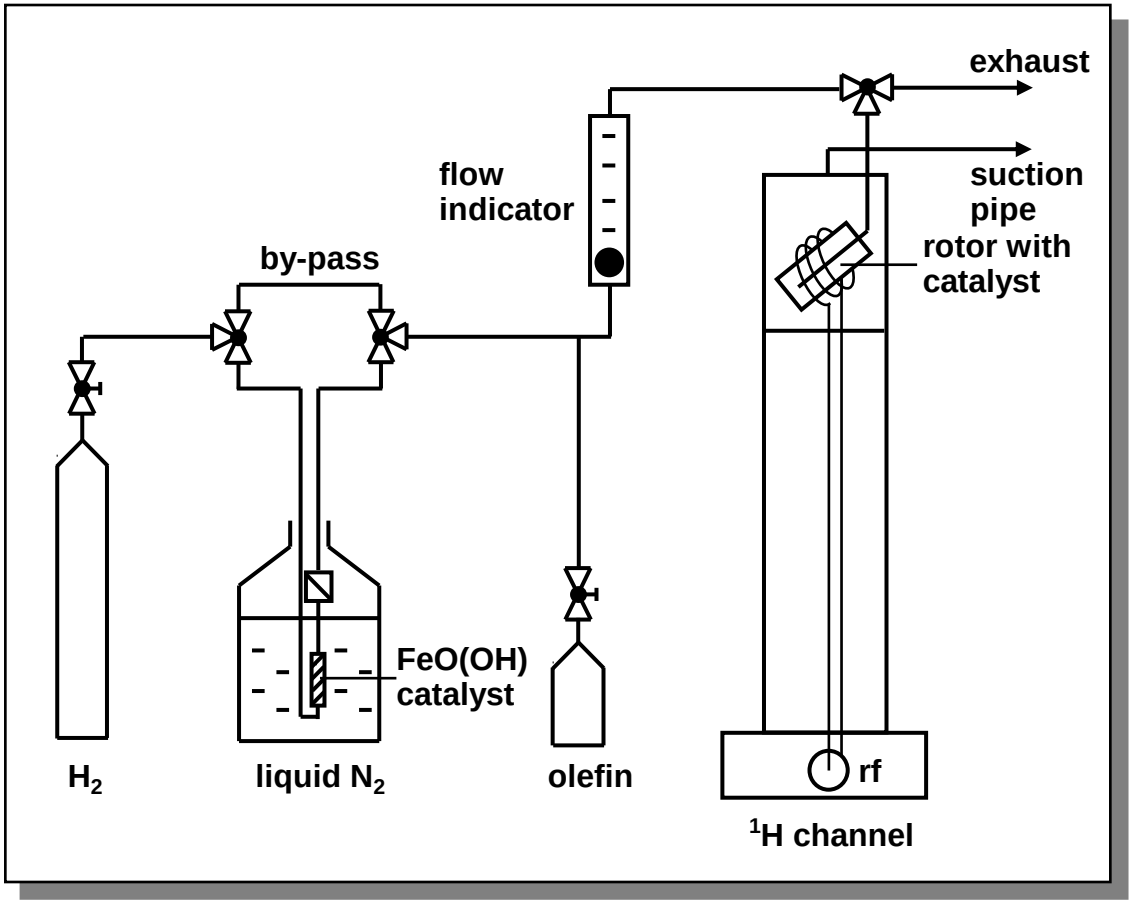

H. Henning et al., Chem. Phys. Lett. 555 (2013) 258.

CF MAS NMR of parahydrogen-induced polarization (PHIP)

PASADENA: Parahydrogen And Synthesis Allow Dramatically Enhanced Nuclear Alignment (p-H_2 incorporation inside the B_0 field)

hydrogenation catalysts:

- zeolite Na-Y (n_{Si}/n_{Al} = 2.7), Degussa AG, Germany, crystal size of ca. 1 µm,
- modification with rhodium(III) chloride hydrate ($RhCl_3 \times H_2O$) for preparing zeolite 0.4[Rh]Na-Y with 0.4 wt.-% Rh (0.5 Rh/u.c.),
- pressed and sieved to particles with diameters of 0.2 to 0.3 mm,
- reduced in flowing hydrogen (100 ml/min) at 653 K for 2 h,
- catalytic experiments performed with 200 and 35 mg of reduced 0.4[Rh]Na-Y (right-hand side).

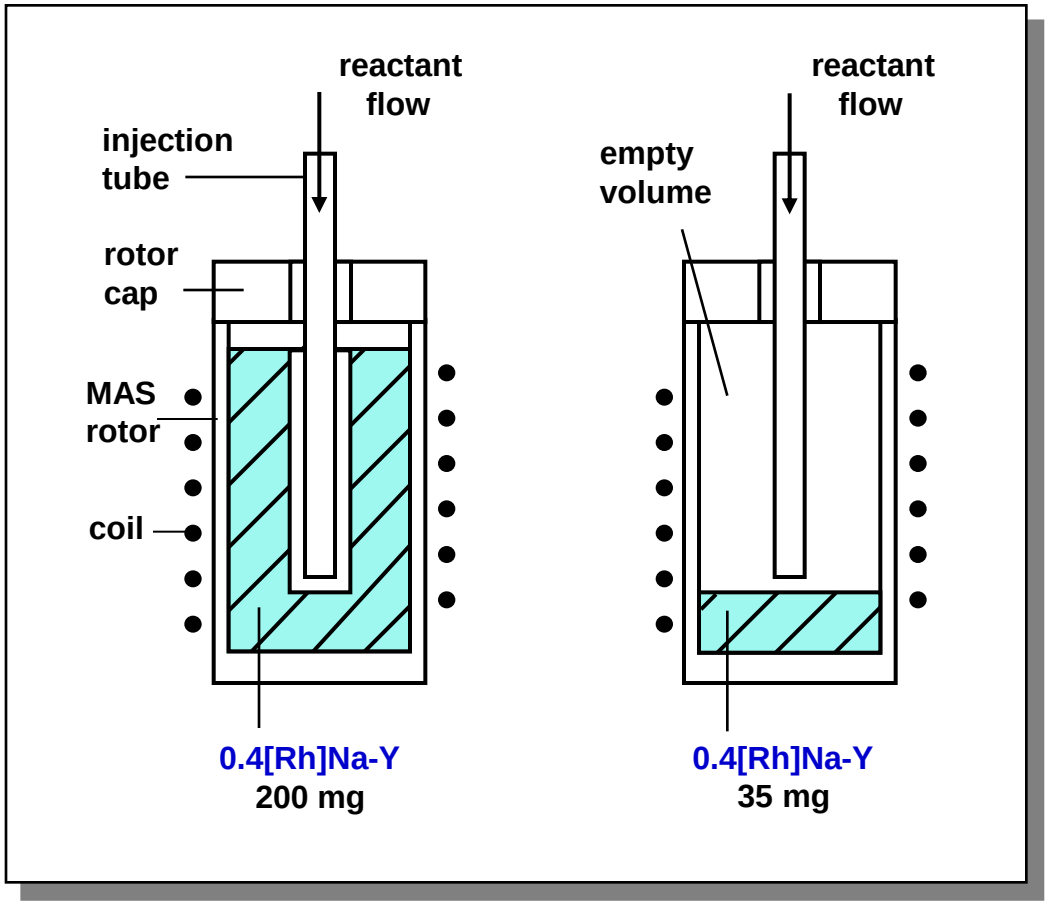

H. Henning et al., Chem. Phys. Lett. 555 (2013) 258.

CF MAS NMR of parahydrogen-induced polarization (PHIP)

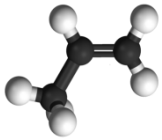

$CH_3-CH=CH_2$ + p-H_2 → (0.4[Rh]Na-Y) → $CH_3-CHH^a-CH_2H^b$

1.72 5.71 4.92 → 0.91 1.33 0.91

^{1}H NMR shift values

***in situ* ^{1}H CF MAS NMR investigation of PHIP at *T* = 295 K**

0.4[Rh]Na-Y (200 mg) + H_2 / propene (1 : 1)

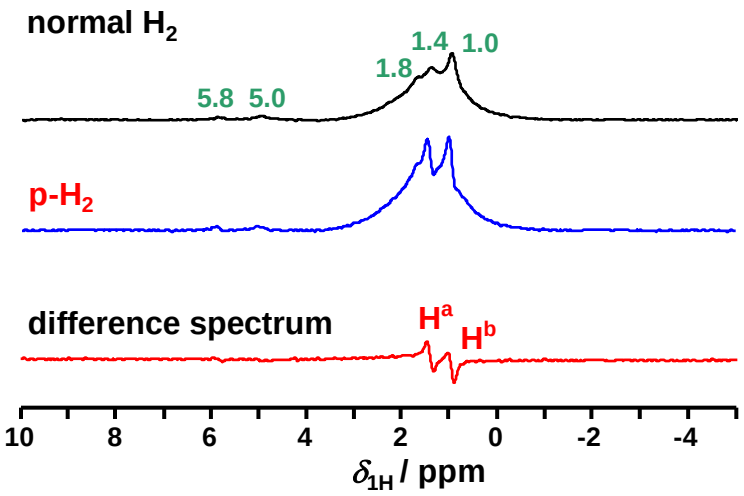

0.4[Rh]Na-Y (35 mg) + H_2 / propene (1 : 1)

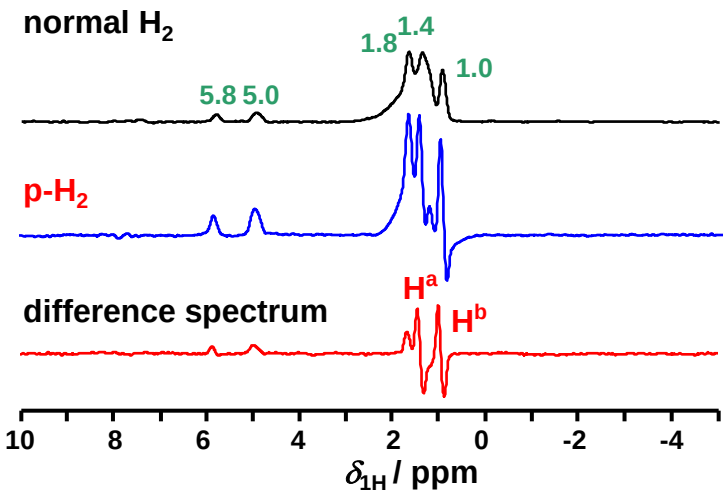

- occurrence of a pairwise incorporation of p-H_2 into propene on zeolite 0.4[Rh]Na-Y
- rapid relaxation of hyperpolarization inside the catalyst bed is a serious limitation

H. Henning et al., Chem. Phys. Lett. 555 (2013) 258.

CF MAS NMR of parahydrogen-induced polarization (PHIP)

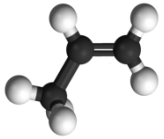

$CH_3-CH=CH_2$ $\xrightarrow[1.0[Pt]TiO_2]{+\ p\text{-}H_2}$ $CH_3-CHH^a-CH_2H^b$

1.36 5.79 4.96 → 0.93 1.36 0.93

^{1}H NMR shift values

***in situ* ^{1}H CF MAS NMR investigation of PHIP at *T* = 340 K**

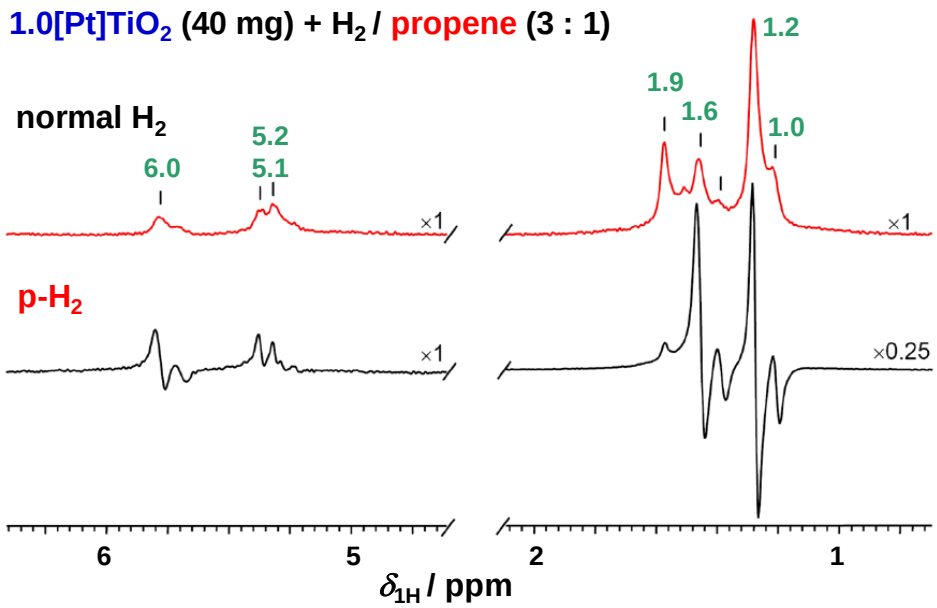

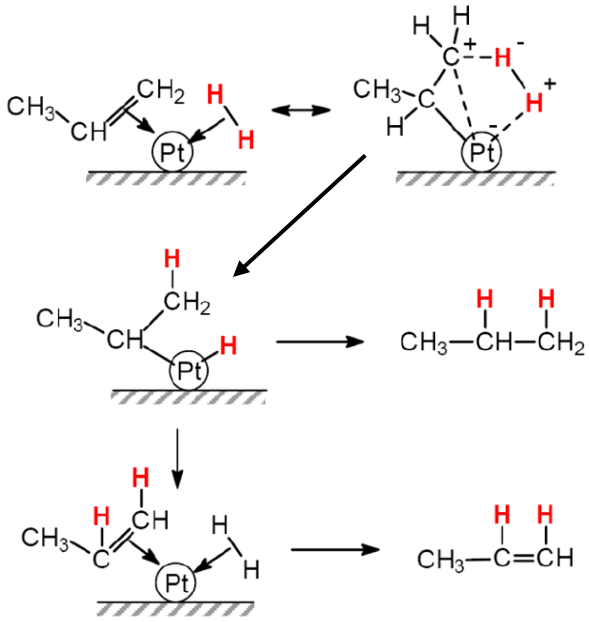

- signals of hyperpolarized ^{1}H nuclei mainly caused by propane in gas phase,
- weak hyperpolarization of propene by selective H/H exchange at C=C double bonds.

S.S. Arzumanov, A.G. Stepanov, J. Phys. Chem. 117 (2013) 2888.

Static NMR of parahydrogen-induced polarization (PHIP)

static ^{1}H NMR investigation of PHIP at T = 403 K

metals and metal oxides + H_2 / 1-butyne

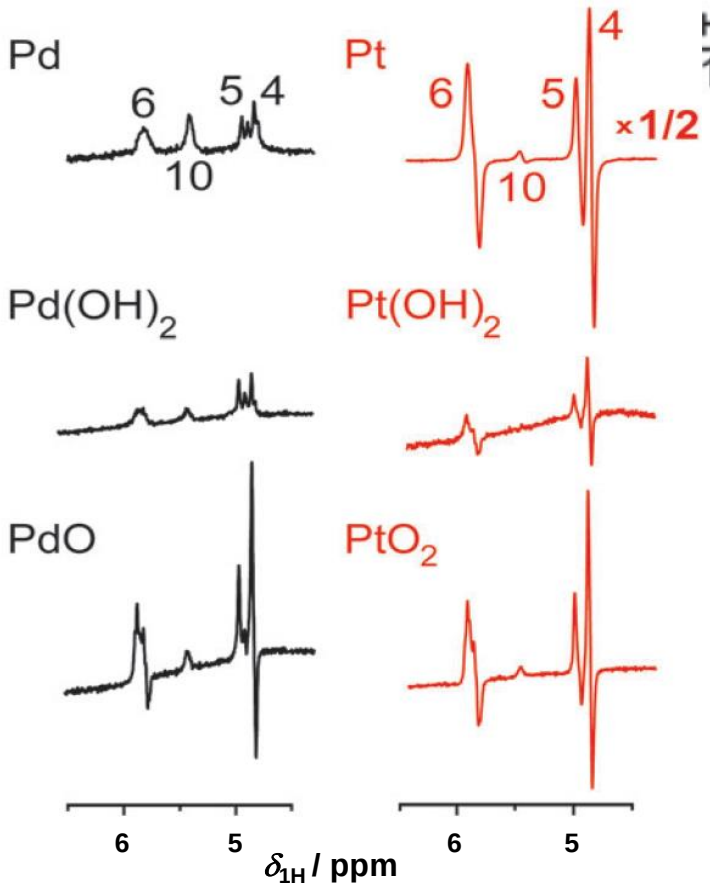

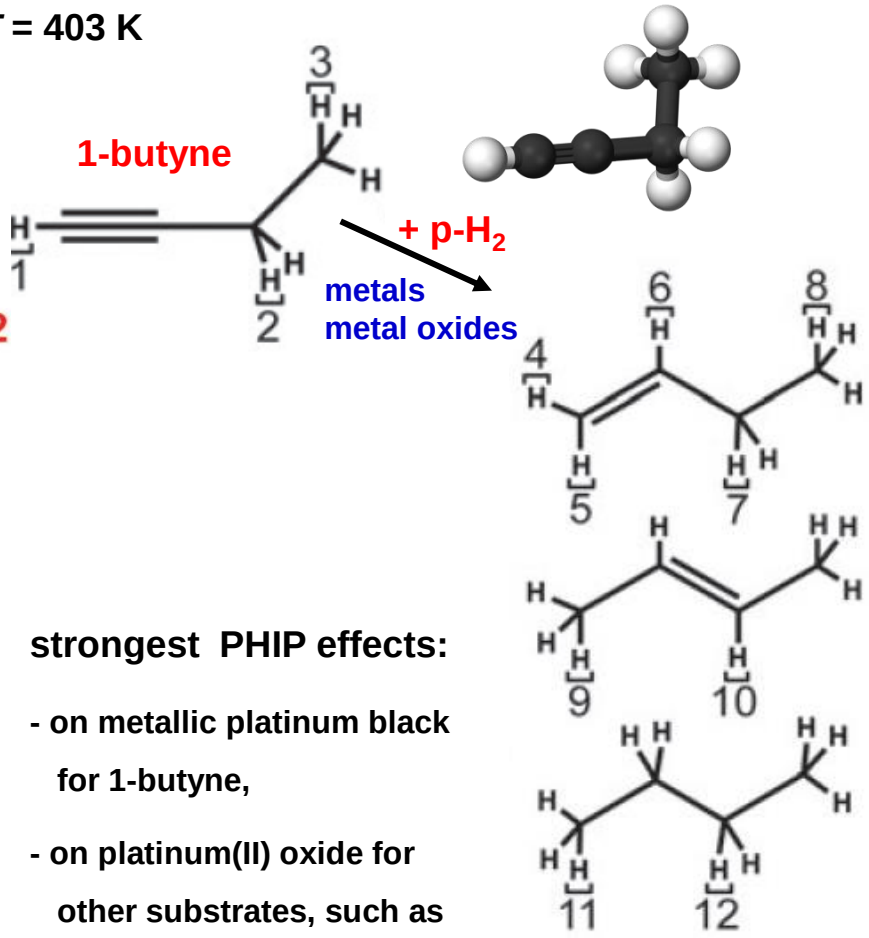

strongest PHIP effects:

- **on metallic platinum black for 1-butyne,**
- **on platinum(II) oxide for other substrates, such as acrolein.**

K.V. Kovtunov et al., Chem. Commun. 50 (2014) 875.

Conditions of PASADENA experiments on solids

- pairwise incorporation of p-H_2 into the reactants is required for reaching hyperpolarization (isolated hydrogenation sites since**?**),
- highly mobile product molecules having low relaxation rate ($\rightarrow$ low number of strong adsorption sites; large pores; sites at outer particle surface; elevated temperature),
- the A_2 spin system must be converted into an AX spin system (chemically non-equivalent H atoms),
- high ratio of $\Delta\omega/J$ improves the observability of the anti-phase signals,
- excitation by $\phi = \pi/4$ pulses because of the density operator

$$\rho(\phi) \propto \cos(\phi)\sin(\phi) \cdot \mathcal{F}(I_1,I_2)$$

- no gaseous oxygen in the flow system (O_2 is paramagnetic; causes p-H_2 to o-H_2 conversion; relaxation of hyperpolarized reactants),
- p-H_2 : reactant ratio of > 1 and elevated temperature may accelerate hydrogenation with p-H_2,
- signal intensity has no explicite dependence on T inside the NMR probe since the enhancement factor

$$\eta = kT\,(1 - 4a)\,/\,(6\gamma_{det}\,\hbar\,B_0)$$

leads to an intensity proportional to $N\gamma_{det}^{3/2}B_0^{1/2}$ (a: p-H_2 content, γ_{det}: γ of detected nuclei)

Thanks to ….

co-workers:

Thomas Horvath
Michael Seiler
Andreas Buchholz
Udo Schenk
Mingcan Xu
Jiang Jiao
Jun Huang
Yijiao Jiang
Jörg Frey
Arne Bressel
Reddy Marthala
Bejoy Thomas
Wei Wang
Yean Sang Ooi
Harald Henning
Weili Dai
Zichun Wang

financial support:

Deutsche Forschungs-gemeinschaft

Fonds der Chemischen Industrie

National Natural Science Foundation of China

Volkswagen Foundation

DECHEMA e.V.

Alexander von Humboldt-Foundation

Thanks to ….